Research Square

Preprints are preliminary reports that have not undergone peer review.
They should not be considered conclusive, used to inform clinical practice,
or referenced by the media as validated information.

The hidden limits of food system resilience under repeated climate shocks in sub-Saharan Africa

Yangfen Chen

chenyangfen@caas.cn

Chinese Academy of Agricultural Sciences

Edwin Mumah

Institute of Agricultural Economics and Development, Chinese Academy of Agricultural Sciences

Jieyong Wang

Institute of Geographic Sciences and Natural Resources Research, Chinese Academy of Sciences (CAS) https://orcid.org/0000-0002-8809-9759

Ren Yang

School of Geography and Planning, Sun Yat-sen University

Shuang Peng

Agricultural Information Institute, Chinese Academy of Agricultural Sciences

Yujia Lu

School of Economics & Management, Northwest University

Wei Wang

Institute of Agricultural Economics and Development, Chinese Academy of Agricultural Sciences

Yu Hong

Institute of Agricultural Economics and Development, Chinese Academy of Agricultural Sciences

Article

Keywords: Food system resilience, Climate shocks, Sub-Saharan Africa, threshold detection, Food security

Posted Date: June 9th, 2026

DOI: https://doi.org/10.21203/rs.3.rs-9945842/v1

License: This work is licensed under a Creative Commons Attribution 4.0 International License.
Read Full License

Additional Declarations: There is **NO** Competing Interest.

The hidden limits of food system resilience under repeated climate shocks in sub-Saharan Africa

Edwin Mumah[a], Jieyong Wang[b], Ren Yang[c], Shuang Peng[d], Yujia Lu[e], Wei Wang[a], Yu Hong[a], Yangfen Chen[a]

Abstract

Food systems in sub-Saharan Africa are increasingly exposed to severe climate shocks, yet the point at which resilience fails remains unclear. We test a limits-to-resilience hypothesis using a balanced panel of 32 countries from 1990 to 2023, combining a Food System Resilience Index (FSRI) with five dimensions of shock exposure to identify the shock intensity at which FSRI no longer buffers undernourishment. We identify a resilience threshold at 30% population affected by droughts or floods (95% CI: 24–36%), below which FSRI reduces undernourishment, and above which protection disappears. Resilience erodes non-linearly, and repeated shocks impose a substantial hidden burden: observed undernourishment exceeds the no-shock counterfactual by 3.5 percentage points, equivalent to 18 million additional undernourished people per year. Eastern and Central Africa, including Somalia, Zambia and the Democratic Republic of the Congo, show the highest combined exposure, low resilience and severe food insecurity. The threshold is stable across time, geography and alternative nutritional outcomes, including child stunting. These findings identify a measurable limit to food system resilience and support proactive, tiered interventions before coping capacity is exhausted.

Keywords: Food system resilience; Climate shocks; Sub-Saharan Africa; threshold detection; Food security.

Food systems face increasing pressure from repeated climate shocks. Extreme weather events are growing in frequency and severity, and successive droughts or floods often strike before food systems can recover[1,2]. Climate risk emerges not from isolated extremes, but from compounding shocks that undermine food availability, affordability, and dietary quality[1,3]. Recent crises highlight this shift. In the Horn of Africa, a prolonged drought shifted directly into flooding in 2023–2024, affecting over 30 million people without recovery time[4]. Such back-to-back shocks, rather than single events, now define food system stress in sub-Saharan Africa (SSA). Despite efforts to build resilience through redundancy and decentralisation, food insecurity more than doubled between 2023 and 2024, reversing gains made since 2000[5,6].

In SSA, weak resilience has worsened food insecurity. The region hosts 307 million undernourished people, or 20% of its population, and nearly 60% of the world's chronically hungry people live there[7-9]. Structural constraints deepen this exposure. About 95% of cropland is rain-fed, and smallholder farmers remain largely excluded from irrigation, credit, and input markets[10,11]. As a result, shocks increasingly arrive in rapid succession and often overlap before recovery is complete, including droughts followed by floods and climate shocks intersecting with conflict and other crises[12]. These conditions suggest that resilience may have limits beyond which it can no longer protect nutritional outcomes.

Current frameworks inadequately capture how food systems break down under recurrent climate shocks. Recovery between shocks is often assumed but fails when disturbances outpace recovery[12,13], and the specific conditions for resilience breakdown are still not well understood. Three gaps remain. First, frameworks assume linear responses,

overlooking nonlinear dynamics where compounding shocks can trigger abrupt collapse[14,15]. Second, they conflate distinct dimensions of shock exposure, obscuring the roles of sequencing and recovery time in shaping food insecurity[16]. Third, resilience thresholds remain poorly defined, especially in low-income settings[17,18]. Together, these gaps limit our ability to identify when resilience weakens, how failure unfolds, and who is most exposed under recurrent shocks.

Here we test a limits-to-resilience hypothesis using a Food System Resilience Index (FSRI) and five dimensions of shock exposure in 32 SSA countries from 1990 to 2023. The framework is designed to identify when resilience weakens under recurrent stress and to quantify the hidden burden of repeated shocks. By linking multidimensional shock exposure to a threshold-based resilience measure, we provide a framework for detecting when food systems begin to fail under cumulative climate stress. This is especially urgent as current trajectories suggest that SDG 2 will not be met by 2030, with climate shocks eroding past gains[9,19]. In the context of widening funding gaps, targeted adaptation is critical to protect vulnerable populations in SSA and beyond.

Results

A critical resilience threshold under recurrent shocks

The protective effect of FSRI on undernourishment disappears above a critical shock intensity. When the proportion of the population affected by droughts or floods in a given year reaches 30% (95% CI: 24–36%; Fig. 1a), the effect of FSRI on undernourishment is no longer significant.

Risk rises quickly with repeated shocks. In low-FSRI countries, the predicted probability of severe food insecurity (PoU >30%) reaches 0.50 after 14 shocks within five years (Fig. 1b). At the same frequency, the probability is 0.27 for countries with mean FSRI and 0.22 for those with high FSRI. The interaction between FSRI and shock frequency is significant ($p < 0.001$), showing that higher resilience delays, but does not stop, risk accumulation.

Vulnerability is geographically concentrated. Somalia, Zambia, and the Democratic Republic of the Congo show triple vulnerability, defined by high shock exposure, low FSRI, and high PoU (Fig. 1c). These countries cluster in Eastern and Central Africa. A similar threshold appears for child stunting. The protective effect of FSRI becomes non-significant at a shock intensity of 28%, close to the estimate for undernourishment (Extended Data Table 1; Extended Data Fig. 5b). In low-FSRI countries, the probability of severe stunting approaches 0.50 after 13.2 shocks within five years. This level is not reached in countries with mean or high FSRI (Extended Data Table 1; Extended Data Fig. 3c).

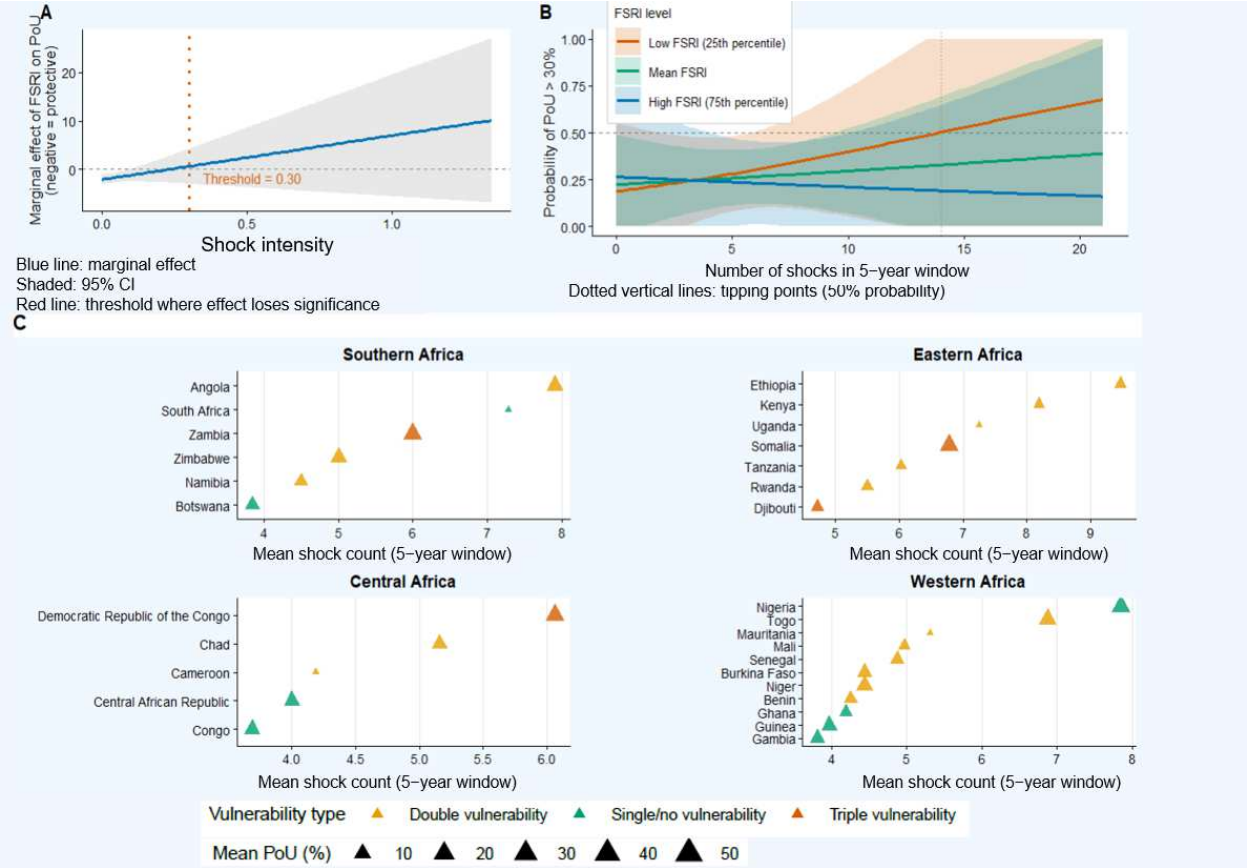


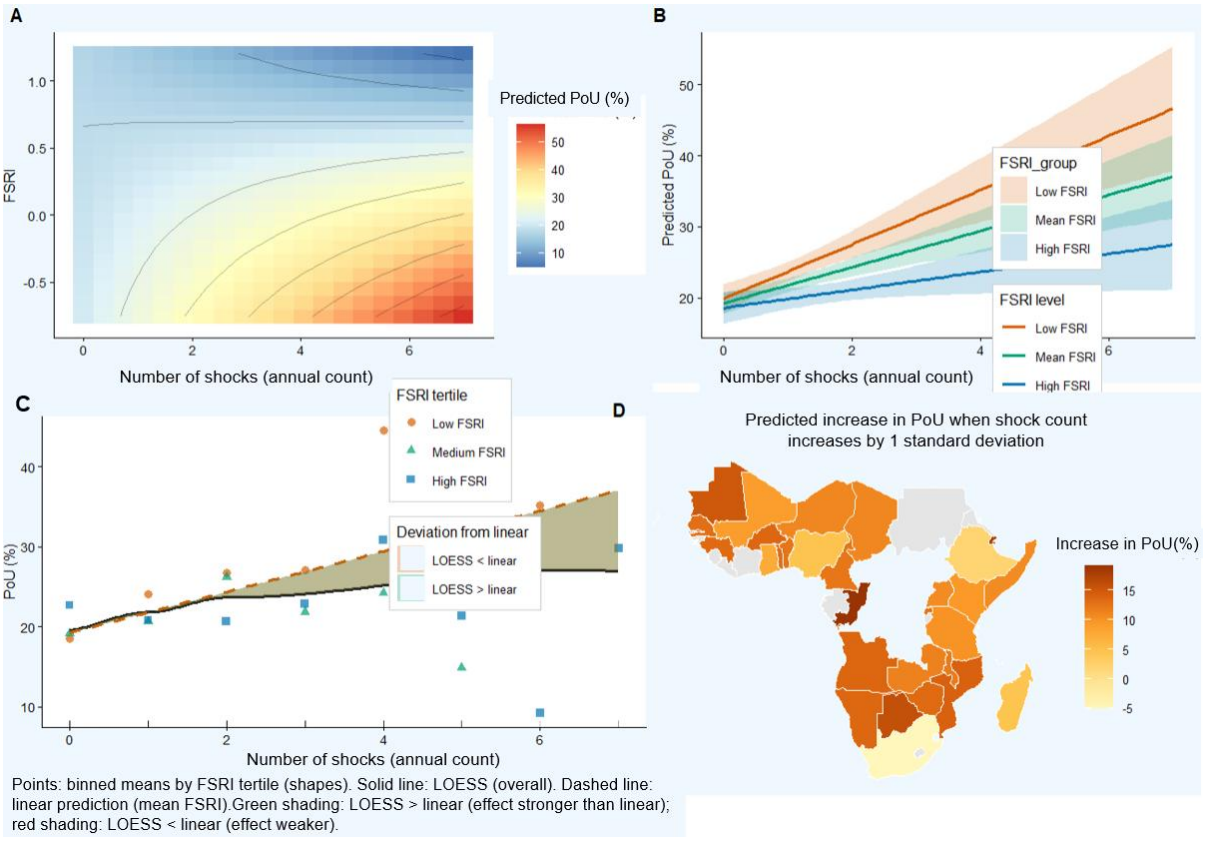
Fig. 1| A critical resilience threshold under recurrent shocks. a, Marginal effect of the FSRI on the PoU across shock intensity. Blue line shows point estimate; grey ribbon indicates 95% confidence interval. The vertical red dotted line marks the shock intensity of 0.30 (30% of the population affected) – the point above which the protective effect of FSRI is no longer statistically significant. b, Probability of severe food insecurity (PoU >30%) as a function of shock frequency over a 5-year window, for low (25th percentile), mean and high (75th percentile) FSRI. Curves show logistic regression predictions with 95% confidence bands; dotted vertical lines indicate the 50% probability tipping points. c, Country-level mean shock frequency (5-year window) and mean PoU for four SSA regions. Points are triangular; colour indicates triple, double or single/no vulnerability (based on exceedance of critical thresholds. Estimates are derived from linear and logistic mixed-effects models using panel data from 1990 to 2023 across 32 SSA countries (n=1,088 after excluding missing values).

Resilience erodes nonlinearly under repeated shocks

Resilience weakens as shocks accumulate. The interaction between annual shock frequency and FSRI is negative and significant ($\beta = -0.33$, $p < 0.001$; Extended Data Table 2), meaning that the protective effect of FSRI diminishes with each additional shock. Each additional shock increases undernourishment, but the size of the increase depends on resilience. At mean FSRI, PoU rises by 1.82 percentage points per shock. The increase is 3.2 percentage points in low-FSRI countries and 0.9 percentage points in high-FSRI countries (Fig. 2b).

The protective effect declines at higher shock frequencies. Contour lines flatten in the heatmap, indicating diminishing returns to resilience (Fig. 2a). The LOESS curve diverges from the linear fit beyond four shocks per year, showing that impacts accelerate at higher frequencies and are not fully captured by a linear specification (Fig. 2c).

This pattern varies across countries. A one-standard-deviation increase in shock frequency raises PoU by 28–35% in Somalia and Zambia, but by less than 10% in South Africa (Fig. 2d). The median increase across countries is 18%. The pattern is consistent for child stunting, where the interaction remains negative and significant (β = –0.29; Extended Data Fig. 3a).



Points: binned means by FSRI tertile (shapes). Solid line: LOESS (overall). Dashed line: linear prediction (mean FSRI).Green shading: LOESS > linear (effect stronger than linear); red shading: LOESS < linear (effect weaker).

Fig. 2| Shock–resilience interaction and predicted impacts of increased shock frequency. a, heatmap of predicted prevalence of undernourishment (PoU) across annual shock count and the FSRI. Colour gradient from dark blue (low PoU) to dark red (high PoU); contour lines are isoclines of predicted PoU. b, predicted PoU by shock count for low (25th percentile), mean, and high (75th percentile) FSRI. Lines show marginal effects with 95% confidence bands. c, binned means of PoU (percentage points) for FSRI tertiles (low, medium, high), with a LOESS smooth (solid line) fitted to all data and the linear model prediction for mean FSRI (dashed line). Green shading indicates where the LOESS lies above the linear prediction (effect stronger than linear); red shading indicates where it lies below (effect weaker). d, map showing the predicted percentage increase in PoU when the annual shock count rises by one standard deviation (holding FSRI at the country-specific mean). LOESS, locally estimated scatterplot smoothing. Estimates are based on linear mixed-effects models with country random effects, controlling for GDP per capita. Data cover 1990–2023 across 32 SSA countries (n=1,088 after excluding missing values).

Hidden costs of repeated shocks

Repeated climate shocks are associated with persistently higher undernourishment across SSA (Fig. 3). From 1990 to 2023, observed undernourishment exceeded the no-shock counterfactual by 3.5 percentage points, rising from 21.1% to 24.6% (Fig. 3a, b). This difference corresponds to about 18 million additional undernourished people per year.

The pattern is widespread. Observed prevalence exceeds the counterfactual in nearly all countries (Fig. 3c). The largest gaps are concentrated in Eastern and Central Africa (Fig. 3d). Kenya shows the greatest divergence, followed by Congo, Angola and Chad. No country shows a comparable reduction under observed conditions.

Nutritional outcomes show the same pattern. In the absence of shocks, stunting would be 2.9 percentage points lower. This is broadly similar to the counterfactual reduction in undernourishment.

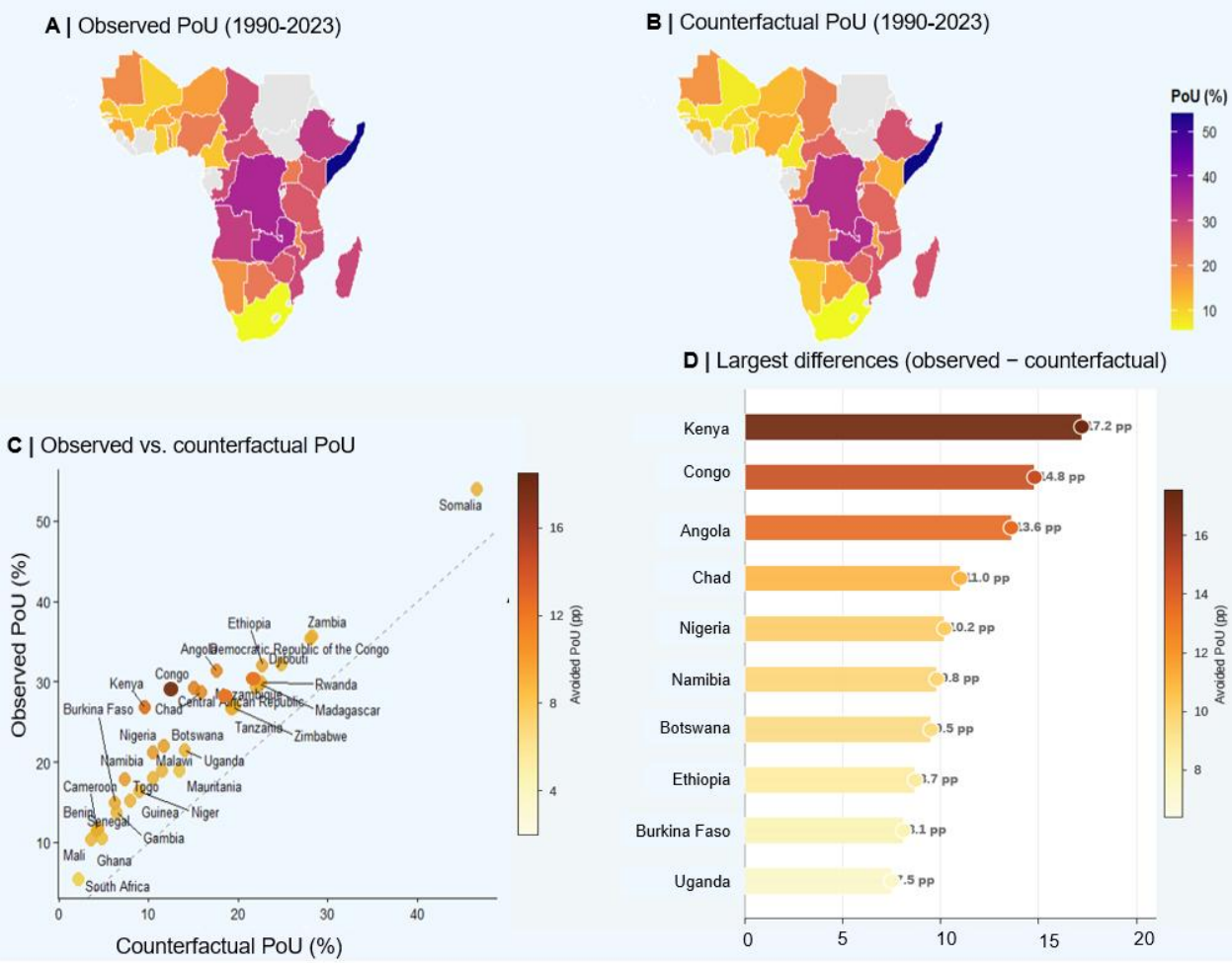


Fig. 3| Counterfactual analysis – the hidden cost of climate shocks. a, Map of average observed PoU across SSA (1990–2023). b, Map of average counterfactual PoU under a scenario of no climate shocks (1990–2023). Both maps use the same colour scale. c, Scatter plot of observed versus counterfactual PoU by country. Points above the 1:1 dashed line indicate that observed undernourishment is higher than the counterfactual; colour shows the magnitude of the difference (avoided undernourishment in percentage points). d, Horizontal bar chart of the ten countries with the largest positive differences (observed > counterfactual), showing where climate shocks have caused the greatest increase in undernourishment. Estimates are derived from the counterfactual model described in the Methods. Data cover 1990–2023 across 32 SSA countries (n=1,088 after excluding missing values).

Extended Data Figs. 2–7 and Supplementary Information sections S1–S5 provide additional analyses, including spatiotemporal trends in resilience, the dynamics of single versus clustered shocks, the contributions of individual

resilience factors, sensitivity of the threshold across time and space, robustness using child stunting, and forward projections to 2050.

Discussion

This study demonstrates that food system resilience in SSA has a measurable but limited buffering effect under repeated climate shocks. FSRI is associated with lower undernourishment at low to moderate shock intensity, but this protection weakens once shocks become too frequent, suggesting that resilience has a conditional threshold rather than a universal effect. More broadly, the results indicate that cumulative exposure and short recovery windows can prevent improvements in resilience from translating into better nutritional outcomes.

Resilience is bounded under repeated climate stress. Food systems can absorb only a finite level of disturbance, and recovery depends not only on shock magnitude but also on the time between events. Beyond a critical intensity, cumulative stress exceeds adaptive capacity, indicating a structural limit rather than a temporary decline in performance. This suggests that resilience depends on both exposure patterns and recovery windows, underscoring the value of threshold-based intervention design.

In SSA, many countries experience shock gaps of less than six months, leaving insufficient time for food systems to recover before the next disturbance strikes. East Africa, as well as parts of Zambia, Malawi, Mozambique, the Central African Republic, and the Democratic Republic of the Congo (DRC), are the regions most affected by co-occurring droughts and heatwaves, as well as consecutive droughts and floods[20]. These regions are home to over 326 million people[21], many of whom are vulnerable to increasingly severe and frequent climate shocks. Under a global warming scenario of 2°C, extreme heat conditions are expected to intensify, with compound extremes projected to increase due to both climate change and rising population exposure[22-24]. As global warming continues, the frequency and intensity of heatwaves, droughts, wildfires, and floods are expected to rise, further undermining resilience[25].

As recovery windows shrink, traditional coping strategies such as accumulating food or assets become less effective. Vulnerable households face not only increased food insecurity but also diminished capacity to invest in productivity-enhancing technologies, thereby perpetuating cycles of poverty[26,27]. This threshold of 30% of the population affected, therefore, serves as a reliable and policy-relevant benchmark, marking the point at which the combination of short recovery periods, compound extremes, and the exhaustion of coping strategies overwhelms the food system's ability to recover. This threshold provides a concrete benchmark for adaptive strategies to build resilience and safeguard food security in the face of escalating climate shocks.

The buffering capacity of food systems collapses when recovery intervals are too short. Rapidly recurring disturbances leave households, markets, and institutions insufficient time to rebuild stocks, restore productive assets, or replenish coping reserves. Even systems with moderately strong resilience indicators experience sharply diminished protection, not due to any single shock, but because cumulative stress erodes recovery opportunities. Resilience thus functions as a dynamic capacity, contingent on the timing and repetition of shocks, rather than a static stock of resources[28,29].

This non-linearity reflects the importance of recovery time in sustaining resilience. When shocks arrive too closely together, households, markets and institutions have insufficient time to rebuild food stocks, restore assets, or replenish coping mechanisms before the next disturbance occurs. As a result, the buffering function of FSRI weakens, not because resilience disappears altogether, but because repeated stress progressively erodes the resources that make recovery possible. This pattern implies a structural limit in resilience rather than a temporary fluctuation, because the constraint arises from the cumulative interaction between disturbance frequency and recovery capacity[30,31].

The pattern is especially relevant in Eastern and Central Africa, where frequent shocks and short recovery windows make this erosion more pronounced[32,33]. In these settings, gains in aggregate FSRI do not necessarily translate into improved nutritional outcomes, because repeated disturbances can overwhelm even moderately strong systems before recovery is complete. This aligns with broader evidence that food systems in high-exposure regions face compounding pressures rather than isolated events, helping explain why resilience gains may stall despite structural improvements[31,34].

Durable food system resilience emerges from interacting capacities. Resilience under repeated shocks depends on a portfolio of complementary mechanisms rather than any single sector. Integrating redundancy, diversity, and social protection, FSRI reflects this multidimensional architecture, offering more robust buffering than isolated gains in GDP or infrastructure. Sector-specific interventions may provide short-term benefits under moderate stress[35], but they are insufficient to prevent cascading failures when shocks recur across production, access, and recovery pathways[36].

This finding reinforces the idea that food system resilience is multidimensional rather than linear or sector-specific[37,38]. Durable resilience emerges when absorptive, adaptive, and transformative capacities reinforce one another, instead of relying on a single indicator of development or physical capacity. In that sense, FSRI is valuable not simply because it is broader, but because it better reflects the interconnected nature of food systems under stress. This helps explain why some systems preserve nutritional outcomes more effectively than others even when exposed to similar climate shocks.

Resilience limits are spatially heterogeneous across sub-Saharan Africa. Eastern and Central African countries including Somalia, Zambia, Rwanda, Madagascar, the Democratic Republic of the Congo, and Congo experience compounded vulnerability due to structural constraints such as reliance on rain-fed agriculture, limited market integration, and pervasive undernourishment[39-41]. In these settings, low resilience reflects not only current shock pressure but also longer-term structural constraints on recovery.

By contrast, countries in Western and Southern Africa, along with some nations in Eastern Africa such as Kenya and Ethiopia, exhibit more heterogeneous resilience trajectories. Some of these countries perform relatively well in both resilience and food security, highlighting that resilience limits are context-dependent rather than uniform. Regional averages can mask substantial country-level differences, and pre-existing structural conditions critically shape how repeated shocks translate into nutritional decline, rendering some food systems far more fragile than others under comparable exposure.

Anticipatory policies are essential to prevent resilience failure. The cost of inaction is substantial: without climate shocks, undernourishment would be markedly lower, and the gap widens as shocks intensify. Repeated disturbances impose cumulative burdens that conventional policy responses are ill-suited to address[42]. The identified threshold 30% of the population affected provides a clear basis for proactive, targeted interventions.

This threshold supports a tiered policy response. below 20%, standard resilience-building (irrigation, market integration, social protection) remains effective; between 20% and 30%, adaptive strategies (livelihood diversification, contingency reserves, shortened response times) are needed; above 30%, transformative interventions (humanitarian relief, migration support, fundamental restructuring) become unavoidable. Three proactive actions follow directly from this threshold. First, pre-arranged contingency finance should be triggered automatically when monitored shock intensity exceeds 25%, bypassing slow humanitarian appeals[43,44]. Second, inter-shock recovery planning must be mandated to extend effective gaps between successive disturbances beyond six months the current median in Eastern Africa[45,46]. Third, regional risk pools (modelled on the African Risk Capacity) should incorporate the 30% threshold into their payout triggers[47,48]. Reducing shock frequency through mitigation can ease pressure, but adaptation that proactively uses the threshold to differentiate interventions will determine whether food systems can withstand escalating climate stress[49,50]. In triple-vulnerability hotspots where high shock exposure, low resilience and high undernourishment coincide threshold identification can guide the timing, scale and location of investments in social protection, irrigation and early warning systems.

However, this study has limitations. National-level data may obscure sub-national variation in resilience and shock exposure. Armed conflict and policy shifts, which we did not account for, could confound the relationship between climate shocks and food security. Our projections assume linear socioeconomic trends, an assumption that may fail during extreme crises. Despite these constraints, the core findings a quantifiable resilience threshold and the hidden cost of repeated shocks remain robust. Future work should integrate household-level data and routinely include child stunting as a cross-validation metric to test the generalizability of the framework across nutritional indicators.

Methods

Data. This study uses a balanced panel of 32 sub-Saharan African countries from 1990 to 2023 to examine the effects of repeated climate shocks. The sample covers about 85% of the region's population and was restricted to countries with complete data for all core variables. The starting year of 1990 captures the period when climate shocks began to intensify more visibly across the region[51,52]. SSA provides a critical context for testing food system resilience due to its high vulnerability to climate variability and underlying structural weaknesses.

Data were drawn from three main sources. Climate shock information on droughts and floods came from EM-DAT, food security data on the prevalence of undernourishment were obtained from FAOSTAT, and socioeconomic and agricultural covariates, including GDP per capita, irrigated land, agricultural value added, infrastructure, and cereal imports, were taken from the World Bank Development Indicators. All variables were harmonized to the country-year level. Data quality was checked through temporal consistency tests, outlier screening, and comparison with national statistics.

We performed temporal consistency checks, outlier detection and cross-validation against national statistics. Missing values in continuous covariates (<5% of observations) were imputed using linear interpolation. To test robustness, we repeated all analyses using last-observation-carried-forward and multiple imputation. Summary statistics were nearly identical across methods (e.g., mean GDP per capita ranged from 2.864 to 2.866; mean FSRI from –0.272 to –0.270), confirming that the results are not sensitive to the imputation technique[53].

Analytical framework: Our analytical framework treats food systems as complex, interconnected systems rather than isolated production sectors[54,55]. It follows recent work showing that repeated stressors can be measured across multiple dimensions and linked to system outcomes in a structured way[56,57], and it combines composite resilience indicators with annual nutritional outcomes to assess how recurrent shocks reshape food-system performance[58].

The framework has three linked components. First, we characterize repeated climate shocks using five complementary metrics: event count, intensity, clustering, inter-event gap, and five-year cumulative exposure. Together, these measures distinguish different dimensions of disturbance that are often collapsed into a single indicator. Second, we estimate resilience with a composite FSRI based on agricultural productivity, economic capacity, physical infrastructure, market access, and social protection. Third, we test for a resilience threshold by identifying the shock intensity at which the protective effect of FSRI on undernourishment becomes statistically indistinguishable from zero.

This design improves on existing approaches in three ways. It allows the effect of resilience to vary with shock burden rather than assuming a constant relationship. It makes the threshold itself empirically observable, which helps identify where resilience begins to fail across contexts. It also translates the threshold into information that is directly relevant for interpretation, by showing where repeated shocks generate the largest hidden burden and where risk concentrates most strongly.

The FSRI captures five domains that reflect core dimensions of food-system resilience: agricultural productivity, economic capacity, physical infrastructure, market access, and social protection. These domains represent a system's ability to absorb, adapt to, and recover from repeated shocks. Agricultural productivity reflects diversification and buffering capacity, economic capacity captures room for financial response, physical infrastructure reflects robustness and connectivity, market access captures spatial reallocation, and social protection reflects institutional support for recovery.

All indicators were harmonized to the country-year level and standardized using z-scores before aggregation. Principal component analysis was then used to derive empirical weights, with the first principal component taken as the FSRI[59]. Higher FSRI values indicate stronger resilience.

Threshold detection: We identified the resilience threshold using a bootstrap-based procedure. We first estimated the interaction model relating undernourishment to shock exposure, FSRI, and their interaction, and then computed the marginal effect of FSRI across the observed range of shock intensity. The threshold was defined as the point at which the 95% confidence interval of the marginal effect crossed zero.

To quantify uncertainty, we resampled the data with 1,000 bootstrap replicates drawn at the country level, preserving panel structure[60]. For each replicate, we re-estimated the model, recalculated the marginal effects and recorded the threshold. The bootstrap distribution of threshold estimates yielded 95% confidence intervals. This approach provides a robust estimate of the shock intensity beyond which the protective effect of FSRI is no longer statistically significant.

Conceptual diagram: The analytical logic of the framework is summarized in a conceptual diagram (Extended Data Fig. 1). Shock intensity is defined as the proportion of the population affected by droughts and floods in a given year, ranging from 0 to 1 (0% to 100%). The diagram maps the five-shock metrics (count, intensity, clustering, gap and five-year cumulative exposure) and the construction of the FSRI from five resilience domains. It also shows the interaction-based estimation of conditional effects, the bootstrap threshold detection procedure, and the resulting policy applications (tiered responses, hotspot targeting and counterfactual cost estimates). Together, this flow illustrates how multidimensional shock characterization and empirical threshold identification translate into actionable interventions.

Outcome Variable: The prevalence of undernourishment (PoU) is a standard indicator of chronic food insecurity, measuring the share of the population whose habitual food intake falls below energy requirements[19]. Annual estimates are derived from food balance sheets and household surveys. We selected PoU for three key reasons. First, it directly measures chronic food insecurity, the ultimate nutritional consequence of food system disruptions[5,59]. Second, PoU captures both food availability (production, trade, stocks) and access (incomes, markets, prices)[61,62]. Third, in contrast to production-based metrics, PoU reflects individual-level outcomes, aligning with our focus on human well-being[63]. PoU ranges from 0% to 100%, with annual variation that allows us to assess responses to repeated shocks. This metric operationalizes our limits-to-resilience hypothesis: a food system may sustain production yet fail to mitigate rising undernourishment.

To capture the multidimensional nature of climate shock exposure, we constructed five metrics of shock frequency, intensity, clustering, spacing, and cumulative burden. Shock count measures the annual number of droughts and floods in each country. Shock intensity is scaled by the share of the population affected. Shock clustering identifies years with two or more events, capturing compound shocks. Shock gap measures the interval between successive shocks and reflects recovery time. Five-year shock count captures medium-term exposure through the rolling sum of shocks over the previous five years. Together, these measures separate distinct features of disturbance that are often conflated in composite indices[46,64,65]

The FSRI is a composite measure of a food system's capacity to provide adequate, accessible and nutritious food during disturbances[36]. It operationalizes resilience through two complementary frameworks: the five-capital framework (natural, human, social, financial, manufactured) quantifies assets that enable systems to withstand shocks[66], the four-qualities framework (robustness, redundancy, resourcefulness, rapidity) assesses how effectively these capitals contribute to resilient outcomes[67]. These qualities align with coping, recovery and transformative capacities[68].

The FSRI comprises five domains. Agricultural productivity (crop and livestock diversity) mitigates climate variability through portfolio effects, providing redundancy[69]. Economic capacity (GDP per capita, agricultural value added) provides financial resources for shock absorption and recovery[70]. Physical infrastructure (irrigation, road density, storage) reduces drought vulnerability and enhances market access, representing robustness[71]. Market access (cereal imports, market integration) enables food reallocation between surplus and deficit areas, demonstrating resourcefulness[72]. Social protection coverage measures institutional safety nets that support vulnerable populations during crises, operationalizing rapidity[73].

All indicators were harmonized to country-year level and standardized to z-scores. Principal component analysis (PCA) was used to derive empirical weights; the first principal component (explaining 47% of total variance) serves as the FSRI[74]. The FSRI is standardized across the full sample with mean zero and standard deviation one; higher values indicate greater resilience

FSRI Calculation and Interpretation: The FSRI is derived from the first principal component (PC1), which captures the maximum shared variance among the six standardized resilience indicators. For each country-year observation, the FSRI is computed as:

$$FSRI_{it} = \sum_{j=1}^{6} w_j z_{jit} \quad (1)$$

Where w_j are the loadings from PC1, and z_{jit} are the standardized indicator values (z-scores). This formulation assigns greater weight to indicators that contribute more to the common resilience dimension. Equivalently, with β_j representing the same loadings:

$$FSRI_{it} = \beta_1 Z_{1it} + \beta_2 Z_{2it} + \beta_3 Z_{3it} + \beta_4 Z_{4it} + \beta_5 Z_{5it} + \beta_6 Z_{6it} \quad (2)$$

The resulting FSRI values are standardized across the full sample with a mean of zero and a standard deviation of one; positive values indicate above-average resilience and negative values below-average resilience relative to the regional mean over the study period. Across the 1,088 countries-year observations, the FSRI ranges from –0.76 to 0.84, with higher values signaling greater capacity to sustain food security under climate stress.

Statistical Analysis: We employed linear mixed-effects models (LMMs) with country-specific random intercepts to account for country-level heterogeneity. LMMs are appropriate for panel data as they partition variance into population-level fixed effects and country-specific deviations, addressing unobserved time-invariant heterogeneity and within-country temporal autocorrelation[75]. The base model is:

$$PoU_{it} = \beta_0 + \beta_1 shock_{it} + \beta_2 FSRI_{it} + \beta_3 (shock_{it} \times FSRI_{it}) + X_{it}\gamma + \alpha_i + \epsilon_{it} \quad (3)$$

Where PoU_{it} is the PoU, $shock_{it}$ represents the five-shock metrics (count, intensity, cluster, gap, five-year count), $FSRI_{it}$ is the Food System Resilience Index, X_{it} are time-varying controls (GDP per capita, irrigated land, agricultural value added, infrastructure, cereal imports), α_i are country random effects, and ϵ_{it} is the error term.

To capture non-linear effects and moderation, we extended the model with a quadratic term for shock frequency and an interaction between shock frequency and FSRI:

$$PoU_{it} = \beta_0 + \beta_1 shock_{it} + \beta_2 Shock_{it}^2 + \beta_3 FSRI_{it} + \beta_4 (shock_{it} \times FSRI_{it}) + X_{it}\gamma + \alpha_i + \epsilon_{it} \quad (4)$$

Following Brambor, Clark and Golder[76] the marginal effect of FSRI on PoU in the presence of an interaction term with shock intensity was computed as the partial derivative. This specification acknowledges that the effect of FSRI is conditional on the level of shock intensity. Threshold detection was done by estimating the shock intensity where the 95% confidence interval of the marginal effect crosses zero, using bootstrap resampling 1,000 replicates[77].

$$\frac{\partial \text{PoU}}{\partial \text{FSRI}} = \beta_2 + \beta_3 shock_{it} \quad (5)$$

Tipping point for severe food insecurity. We used logistic regression to predict the probability of severe undernourishment ($PoU_{it} < 30\%$). as a function of five-year shock count, FSRI, and their interaction:

$$\log\left(\frac{p_{it}}{1-p_{it}}\right) = \beta_0 + \beta_1 shockcount5yr_{it} + \beta_2 FSRI_{it} + \beta_3 (shockcount5yr_{it} \times FSRI_{it}) \quad (6)$$

The 50% probability point (tipping point) was calculated for low (25th percentile), mean and high (75th percentile) FSRI values.

Counterfactual analysis. We estimated the prevalence of undernourishment under a "no shocks" scenario by setting all shock variables to zero while keeping other drivers at their observed values:

$$PoU_{it}^{cf} = \beta_0 + \beta_2 FSRI_{it} + X_{it}\gamma + \alpha_i + \epsilon_{it} \quad (7)$$

The difference between observed and counterfactual PoU represents the hidden cost of climate shocks. Uncertainty was assessed with 1,000 bootstrap replicates[78] .

We tested the robustness of the threshold across different time periods (1990–2005, 2006–2023) and geographical regions (Western, Eastern, Central, and Southern Africa) by calculating the threshold from Equation (3) for each subset, with bootstrap confidence intervals (1,000 replicates). All estimates were consistent with the full sample threshold (30%, 95% CI: 24–36%), demonstrating robustness.

For country-level analysis, we computed the mean PoU for the early (1990–2005) and late (2006–2023) periods and visualized changes (ΔPoU) as a bar chart (**Extended Data Fig. 4)**. Positive values indicate worsening, negative values indicate improvement.

Forward-looking projections. To project future risks, we extrapolated socioeconomic drivers (GDP per capita, agricultural value added, FSRI) from historical trends and considered three scenarios: baseline (shocks at pre-1990 levels), a 20% increase in shock frequency, and a 50% increase (**Extended Data Fig. 6)**. These percentages align with IPCC AR6 projections for SSA under high-emission pathways[67,79]. Future PoU was predicted using a fixed-effects panel model (Equation 4) with bootstrapped prediction intervals (1,000 replicates). Population projections from the UN World Population Prospects converted percentages to absolute numbers of undernourished people

Robustness check using child stunting

To assess the robustness of our findings, we replicated the primary analyses using child stunting as an alternative outcome. Stunting, a key indicator of chronic undernutrition, is commonly used in food security and climate impact studies[41,45]. We sourced stunting prevalence data for children under five from the UNICEF/WHO/World Bank Joint Child Malnutrition Estimates (1990–2023), which provides harmonized, model-based annual estimates across 32 countries. These data were integrated with our existing panel.

All core models; interaction, threshold, logistic tipping points, and counterfactuals were re-estimated with stunting as the dependent variable, while keeping the independent variables and fixed effects consistent. We applied the same analytical procedures and bootstrap uncertainty quantifications. If the results based on stunting align with those obtained using the PoU metric, this would further confirm the robustness of our conclusions, indicating that the choice of nutritional indicator does not drive the observed outcomes.

Reference

1. Reed *et al.* The impact of flooding on food security across Africa. *Proceedings of the National Academy of Sciences* **119**, e2119399119 (2022).
2. Naumann, G., Cammalleri, C., Mentaschi, L. & Feyen, L. Increased economic drought impacts in Europe with anthropogenic warming. *Nature Climate Change* **11**, 485-491 (2021).
3. Burney, J., McIntosh, C., Lopez-Videla, B., Samphantharak, K. & Gori Maia, A. Empirical modeling of agricultural climate risk. *Proceedings of the National Academy of Sciences* **121**, e2215677121 (2024).
4. Brumfield, K. D. *et al.* Climate change and Vibrio: Environmental determinants for predictive risk assessment. *Proceedings of the National Academy of Sciences* **122**, e2420423122 (2025).
5. FAO. The State of Food Security and Nutrition in the World 2025 – Addressing high food price inflation for food security and nutrition. (2025).
6. World Bank. Enhancing Food and Nutrition Security in the Sahel and Horn of Africa. (2024).
7. Pérez-Escamilla, R., Salles-Costa, R. & Segall-Corrêa, A. M. Food insecurity experience-based scales and food security governance: A case study from Brazil. *Global Food Security* **41**, 100766 (2024).
8. Itoh, H., Yamashita, H., Wada, K. C. & Yonemaru, J.-i. Real-time emulation of future global warming reveals realistic impacts on the phenological response and quality deterioration in rice. *Proceedings of the National Academy of Sciences* **121**, e2316497121 (2024).
9. FAO. Uganda Flags Off First-Ever Shipment of Dried Chili to China. (2025).
10. Thornton, P. K. & Herrero, M. Adapting to climate change in the mixed crop and livestock farming systems in sub-Saharan Africa. *Nature Climate Change* **5**, 830-836 (2015).
11. Chrisendo, D. *et al.* A systematic review of sustainable food systems identifies socio-economic pathways driving food systems transformations. *Nature food*, 1-13 (2026).
12. McCool, W. C. *et al.* Modeling the rise and demise of Classic Maya cities: Climate, conflict, and economies of scale. *Proceedings of the National Academy of Sciences* **122**, e2512325122 (2025).
13. Amorim-Maia, A. T. & Olazabal, M. Beyond adjustment: a new paradigm for climate change adaptation in a complex world. *Global Environmental Change* **93**, 103027 (2025).
14. Scheffer, M. *et al.* Early-warning signals for critical transitions. *Nature* **461**, 53-59 (2009).

15. Folke, C. *et al.* Resilience thinking: integrating resilience, adaptability and transformability. *Ecology and society* **15** (2010).
16. Cinner, J. E. *et al.* Gravity of human impacts mediates coral reef conservation gains. *Proceedings of the National Academy of Sciences* **115**, E6116-E6125 (2018).
17. Rocha, J. C., Peterson, G., Bodin, Ö. & Levin, S. Cascading regime shifts within and across scales. *Science* **362**, 1379-1383 (2018).
18. Barrett, C. B. & Carter, M. R. The economics of poverty traps and persistent poverty: Empirical and policy implications. *The Journal of Development Studies* **49**, 976-990 (2013).
19. Lentz, E., Baylis, K., Michelson, H. & Kim, C. Official estimates of global food insecurity undercount acute hunger. *Nature Food*, 1-13 (2025).
20. Weber, T. *et al.* Analysis of compound climate extremes and exposed population in Africa under two different emission scenarios. *Earth's Future* **8**, e2019EF001473 (2020).
21. Worldometer. Current World Population. (2022).
22. Harrington, L. J. & Otto, F. E. Changing population dynamics and uneven temperature emergence combine to exacerbate regional exposure to heat extremes under 1.5 C and 2 C of warming. *Environmental Research Letters* **13**, 034011 (2018).
23. De Ruiter, M. C. *et al.* Why we can no longer ignore consecutive disasters. *Earth's future* **8**, e2019EF001425 (2020).
24. Van de Walle, J. *et al.* Future intensification of precipitation and wind gust associated thunderstorms over Lake Victoria. *Weather and Climate Extremes* **34**, 100391 (2021).
25. Mora, C. *et al.* Broad threat to humanity from cumulative climate hazards intensified by greenhouse gas emissions. *Nature climate change* **8**, 1062-1071 (2018).
26. Dzanku, F. M., Jirström, M. & Marstorp, H. Yield gap-based poverty gaps in rural Sub-Saharan Africa. *World Development* **67**, 336-362 (2015).
27. Kotir, J. H. Climate change and variability in Sub-Saharan Africa: a review of current and future trends and impacts on agriculture and food security. *Environment, Development and Sustainability* **13**, 587-605 (2011).
28. McDonald, A. J. *et al.* Time management governs climate resilience and productivity in the coupled rice–wheat cropping systems of eastern India. *Nature Food* **3**, 542-551 (2022).
29. Wang, S., Chen, X. & Han, N. Intelligent development of manufacturing enterprises and supply chain Resilience: A perspective based on internal capabilities and external linkages. *Expert Systems with Applications*, 131338 (2026).
30. Jha, P., Yadav, P. K., Joy, M. S., Bansal, T. & Jha, A. N. Crossing the Ecological Threshold: Spatio-Temporal Dynamics of Blue-Green Space Ecosystem Health in Delhi using a VORR Framework. *Environmental and Sustainability Indicators*, 101243 (2026).
31. Dutta, S. *et al.* Unraveling anthropogenic and climate stressors in the Sundarbans and their ripple effects on livelihoods and ecosystems, and adaptation strategies for a sustainable future–A systematic review. *Environmental Development*, 101410 (2025).
32. Wardekker, A. Building climate resilience in deltas amid uncertainty and surprise. *One Earth* **6**, 200-204 (2023).
33. Douxchamps, S., Debevec, L., Giordano, M. & Barron, J. Monitoring and evaluation of climate resilience for agricultural development–A review of currently available tools. *World Development Perspectives* **5**, 10-23 (2017).
34. Jha, R. *et al.* Global nutritional challenges and opportunities: Buckwheat, a potential bridge between nutrient deficiency and food security. *Trends in Food Science & Technology*, 104365 (2024).

35. Ataei, P., Alinaghizadeh, M., Alibakhshi, H., Valizadeh, N. & Karimi, H. How Is Food Security Threatened in Iran's Agricultural Sector? A Grounded Theory Approach. *Global Transitions* (2026).
36. Tendall, D. M. *et al.* Food system resilience: Defining the concept. *Global food security* **6**, 17-23 (2015).
37. Ma, Y., Li, X. & Luo, Y. Microbiome-driven innovations for climate-resilient crop production. *Nature Food*, 1-5 (2026).
38. Muleke, A. *et al.* Regenerative agriculture improves productivity and profitability while reducing greenhouse gas emissions on Australian sheep farms. *Nature Food*, 1-11 (2026).
39. De Vos, K. *et al.* Rice availability and stability in Africa under future socio-economic development and climatic change. *Nature food* **4**, 518-527 (2023).
40. Cole, M. J., Bailey, R. M. & New, M. G. Tracking sustainable development with a national barometer for South Africa using a downscaled "safe and just space" framework. *Proceedings of the National Academy of Sciences* **111**, E4399-E4408 (2014).
41. Phalkey, R. K., Aranda-Jan, C., Marx, S., Höfle, B. & Sauerborn, R. Systematic review of current efforts to quantify the impacts of climate change on undernutrition. *Proceedings of the National Academy of Sciences* **112**, E4522-E4529 (2015).
42. Ulimwengu, J. M. & Blumenthal, N. Assessing structural failure of African food systems. *Empowering Africa's food systems for the future*, 27-51 (2023).
43. FAO. Anticipating shocks through social protection. (2026).
44. OCHA. Anticipatory Action - Activations in Eastern Africa: January 2024 - December 2025 (as of December 2025)*. United Nations Office for the Coordination of Humanitarian Affairs. Available at:. (2025).
45. FAO. What are healthy diets? Joint statement by the Food and Agriculture Organization of the United Nations and the World Health Organization. . (WHO., Geneva, Switzerland, 2024).
46. Delforge, D. *et al.* EM-DAT: the emergency events database. *International Journal of Disaster Risk Reduction* **124**, 105509 (2025).
47. World Economic Forum. What Africa's climate response experience can teach the world. (2025).
48. Xia, L. *et al.* Global food insecurity and famine from reduced crop, marine fishery and livestock production due to climate disruption from nuclear war soot injection. *Nature Food* **3**, 586-596 (2022).
49. Okoye, C. U. *et al.* Climate-resilient food systems for nutrition security in Sub-Saharan Africa: innovations in sustainable agriculture and policy for vulnerable populations. *Climatic Change* **178**, 202 (2025).
50. Oyadeyi, O. O. & Oyadeyi, O. A. Climate change, green economy, and agriculture-a development pathway towards food security and climate resilient sub-Saharan African countries. *Scientific African* **29**, e02792 (2025).
51. Otsuka, K., Jayne, T. S., Mano, Y. & Takahashi, K. Toward a sustainable Green Revolution in sub-Saharan Africa: The case of maize and rice. *Food Policy* **129**, 102762 (2024).
52. Eissler, S., Thiede, B. C. & Strube, J. Climatic variability and changing reproductive goals in Sub-Saharan Africa. *Global Environmental Change* **57**, 101912 (2019).
53. Chrisendo, D. *et al.* Rising income inequality across half of global population and socioecological implications. *Nature sustainability*, 1-13 (2025).
54. Allan, J. D. *et al.* Joint analysis of stressors and ecosystem services to enhance restoration effectiveness. *Proceedings of the National Academy of Sciences* **110**, 372-377 (2013).

55. Papargyropoulou, E. *et al.* Research framework for food security and sustainability. *npj Science of Food* **9**, 13 (2025).
56. Appiah-Twumasi, M., Gardebroek, C., Ihle, R. & Ansah, I. G. Responses of African food systems to climate change: A systematic review of concepts, methods, and evidence. *Agricultural Systems* **233**, 104577 (2026).
57. Ikuemonisan, E. & Eniafe, O. D. Climate shocks and cumulative vulnerability in Nigeria's small-scale fisheries: evidence on income losses, regressive impacts, and the limits of conventional policy levers. *Journal for Nature Conservation*, 127313 (2026).
58. FAO. Resilient food systems – A proposed analytical strategy for empirical applications. (2021).
59. Schneider, K. R. *et al.* The state of food systems worldwide in the countdown to 2030. *Nature Food* **4**, 1090-1110 (2023).
60. Aparicio, J., Kapelko, M., Monge, J. F. & Zofío, J. L. Enhancing the Benefit of the Doubt model through 'Ensemble-DEA': achieving the Sustainable Development Goals. *Expert Systems with Applications*, 129010 (2025).
61. Hammad, A. T. & Falchetta, G. Probabilistic forecasting of remotely sensed cropland vegetation health and its relevance for food security. *Science of the Total Environment* **838**, 156157 (2022).
62. Sanogo, I. & Amadou, M. M. Rice market integration and food security in Nepal: The role of cross-border trade with India. *Food Policy* **35**, 312-322 (2010).
63. Elsler, L. G. *et al.* Global nutritional equity of fishmeal and aquaculture trade flows. *Proceedings of the National Academy of Sciences* **123**, e2506699123 (2026).
64. Galli, N., Govoni, C. & Rulli, M. C. Assessing the impact of hydrological extremes on food security from post-disaster reporting. *Global Food Security*, 100889 (2025).
65. Demont, T. Coping with shocks: How Self-Help Groups impact food security and seasonal migration. *World Development* **155**, 105892 (2022).
66. Rockström, J. *et al.* The EAT–Lancet Commission on healthy, sustainable, and just food systems. *The Lancet* **406**, 1625-1700 (2025).
67. IPCC. AR6, Chapter 9 on Africa: projects 20–50% increases in drought/flood frequency under high emissions., (2022).
68. Béné, C. Resilience of local food systems and links to food security–A review of some important concepts in the context of COVID-19 and other shocks. *Food security* **12**, 805-822 (2020).
69. Kolapo, A. & Sieber, S. From vulnerability to viability: Climate-Smart agriculture as drivers of productivity and food security in Nigerian maize-based farming households. *Environmental Challenges*, 101268 (2025).
70. Xu, D. *et al.* Quantitative characterization of resilience and analysis of driving mechanisms in the water-energy-food nexus system of major grain-producing regions. *Journal of Hydrology*, 134201 (2025).
71. Carrão, H., Naumann, G. & Barbosa, P. Mapping global patterns of drought risk: An empirical framework based on sub-national estimates of hazard, exposure and vulnerability. *Global Environmental Change* **39**, 108-124 (2016).
72. Cerqueti, R., Montalbano, P., Nenci, S. & Storani, S. Shocks and reconfiguration in global value chains: A complex network perspective on the global south. *World Development* **204**, 107413 (2026).

73. Baldwin-Cantello, W. *et al.* The Triple Challenge: synergies, trade-offs and integrated responses for climate, biodiversity, and human wellbeing goals. *Climate Policy* **23**, 782-799 (2023).
74. Quinn, K. N., Clement, C. B., De Bernardis, F., Niemack, M. D. & Sethna, J. P. Visualizing probabilistic models and data with intensive principal component analysis. *Proceedings of the National Academy of Sciences* **116**, 13762-13767 (2019).
75. Bell, A. & Jones, K. Explaining fixed effects: Random effects modeling of time-series cross-sectional and panel data. *Political Science Research and Methods* **3**, 133-153 (2015).
76. Brambor, T., Clark, W. R. & Golder, M. Understanding interaction models: Improving empirical analyses. *Political analysis* **14**, 63-82 (2006).
77. Efron, B. Estimation and accuracy after model selection. *Journal of the American Statistical Association* **109**, 991-1007 (2014).
78. Hsiang, S. *et al.* Estimating economic damage from climate change in the United States. *Science* **356**, 1362-1369 (2017).
79. Van Dijk, M., Morley, T., Rau, M. L. & Saghai, Y. A meta-analysis of projected global food demand and population at risk of hunger for the period 2010–2050. *Nature food* **2**, 494-501 (2021).
80. Manikas, I., Ali, B. M. & Sundarakani, B. A systematic literature review of indicators measuring food security. *Agriculture & food security* **12**, 10 (2023).

Data availability

The climate shock data (droughts and floods) are available from the EM-DAT database (https://www.emdat.be/). Prevalence of undernourishment data are from FAOSTAT (https://www.fao.org/faostat/). Socioeconomic and agricultural indicators are from the World Bank Development Indicators (https://databank.worldbank.org/). The final panel dataset constructed for this study (country-year level, 1990–2023) is available from the corresponding author upon reasonable request.

Acknowledgements

The authors gratefully acknowledge support from the Science and Technology Innovation Project of the Chinese Academy of Agricultural Sciences (CAAS-CSAERD-202402; 10-IAED-RC-11-2026; 10-IAED-04-2026), the National Natural Science Foundation of China (72073129), and the National Social Science Foundation of China (21&ZD093).

Author information

[a] Institute of Agricultural Economics and Development, Chinese Academy of Agricultural Sciences, Beijing 100081, China

[b] Institute of Geographic Sciences and Natural Resources Research, Chinese Academy of Sciences, Beijing 100101, China

[c] School of Geography and Planning, Sun Yat-sen University, Guangzhou 510006, China

[d] Agricultural Information Institute, Chinese Academy of Agricultural Sciences, Beijing 100081, China

[e] School of Economics & Management, Northwest University, Xi'an 710127, China

Correspondence to Yangfen Chen (chenyangfen@caas.cn)

Author contributions

E.M., Y.C. and J.W. designed and conceptualised the study. R.Y., Y.L. and W.W. supported data collection and stakeholder engagement. Y.H. and S.P. developed statistical methods and performed the analyses and visualisations. E.M., Y.C. and J.W. wrote the first draft. All authors reviewed and approved the final paper. Y.C. supervised the work.

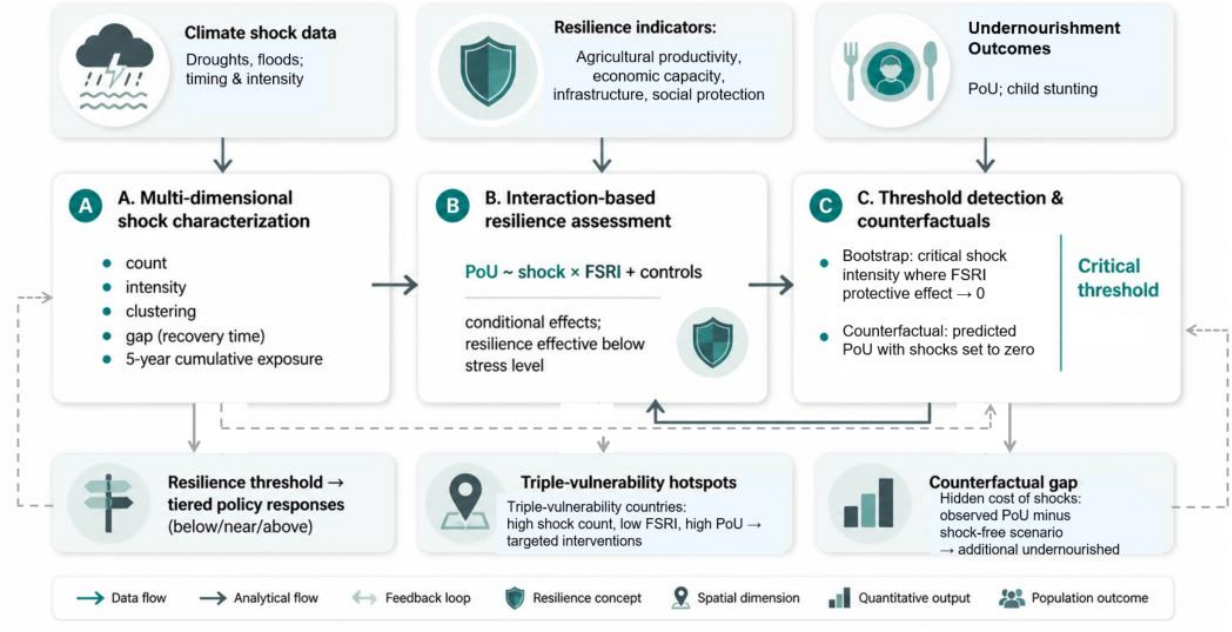
Competing interests

The authors declare no competing interests.

Declaration of generative AI and AI-assisted technologies in the writing process

During the preparation of this work, the authors used ChatGPT-5.1 to improve editing, readability, and language quality. After using this tool, the authors reviewed and revised the content as needed and take full responsibility for the final manuscript.

Extended Data figures and tables

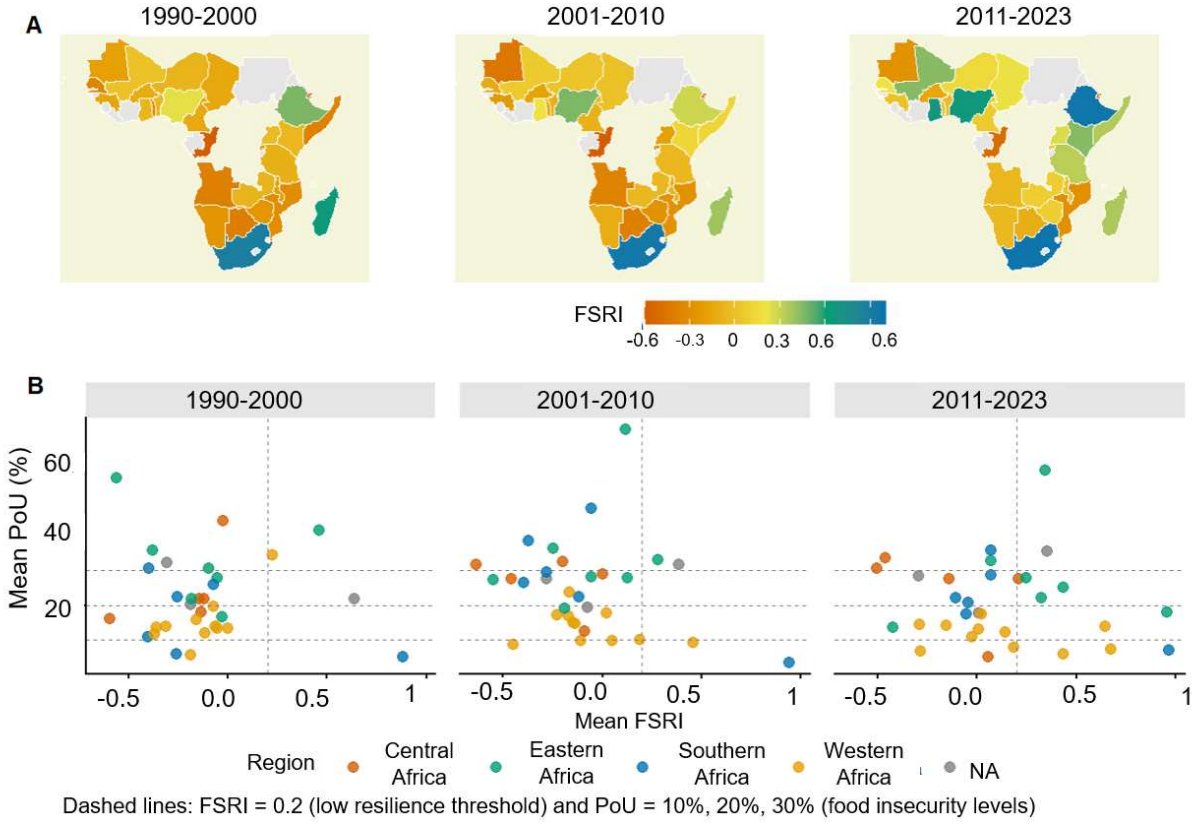


Extended Data Fig. 1| Analytical framework for assessing limits to food-system resilience under repeated climate shocks.

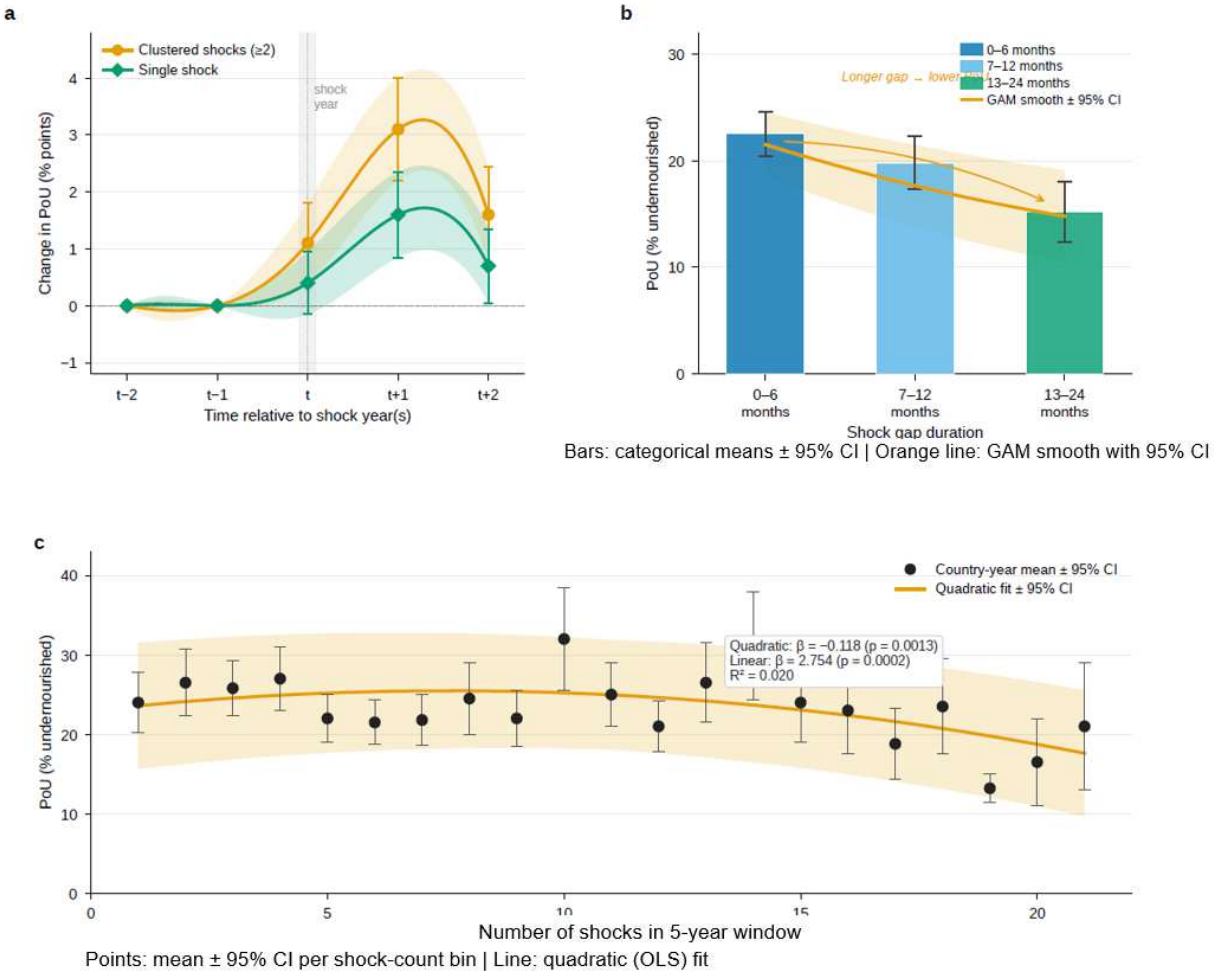
Extended Data Table 1| FSRI components and weighting

Domain	Indicator(s)	Role in FSRI	Standardization	Weighting approach
Agricultural productivity	Crop and livestock diversity	Captures production diversification and buffering capacity	Z-score standardization	First principal component
Economic capacity	GDP per capita; agricultural value added	Reflects financial resources for absorption and recovery	Z-score standardization	First principal component
Physical infrastructure	Irrigation coverage; road density; storage capacity	Captures robustness and market connectivity	Z-score standardization	First principal component
Market access	Cereal imports; market integration	Reflects spatial food reallocation capacity	Z-score standardization	First principal component
Social protection	Social protection coverage	Captures institutional buffering and recovery support	Z-score standardization	First principal component

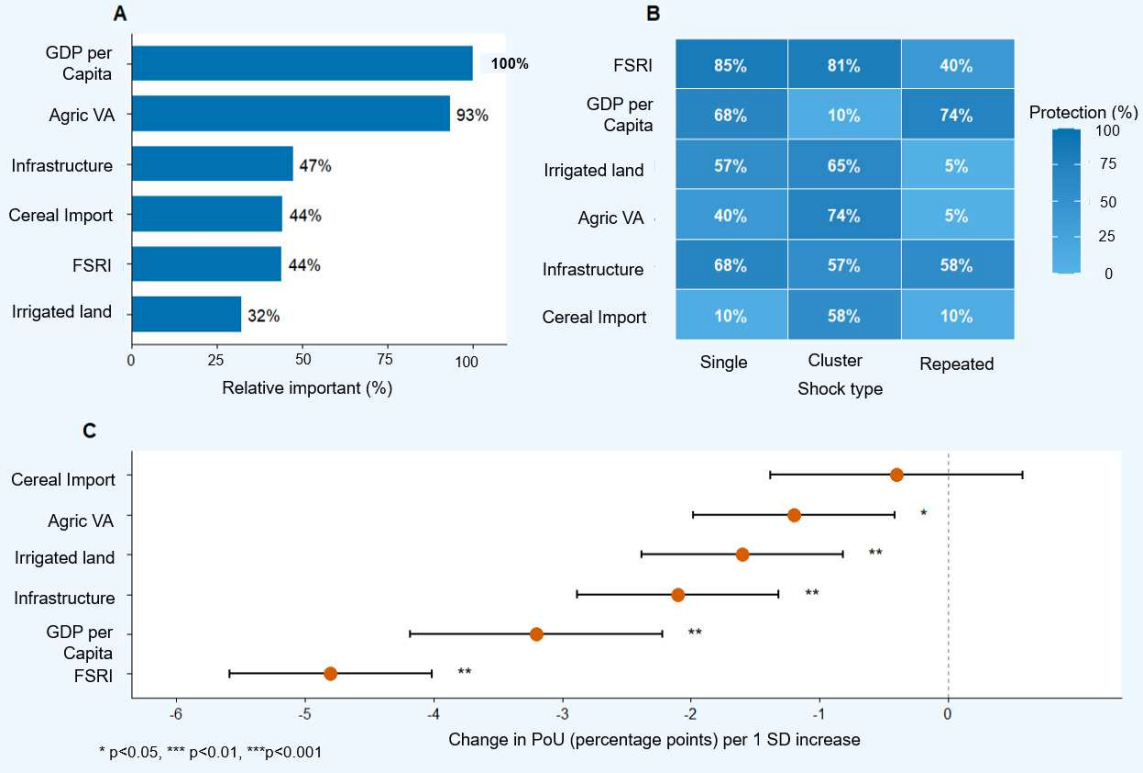
Note: All indicators were harmonized to the country-year level before standardization. The FSRI was extracted from the first principal component, with larger values indicating stronger resilience [80].



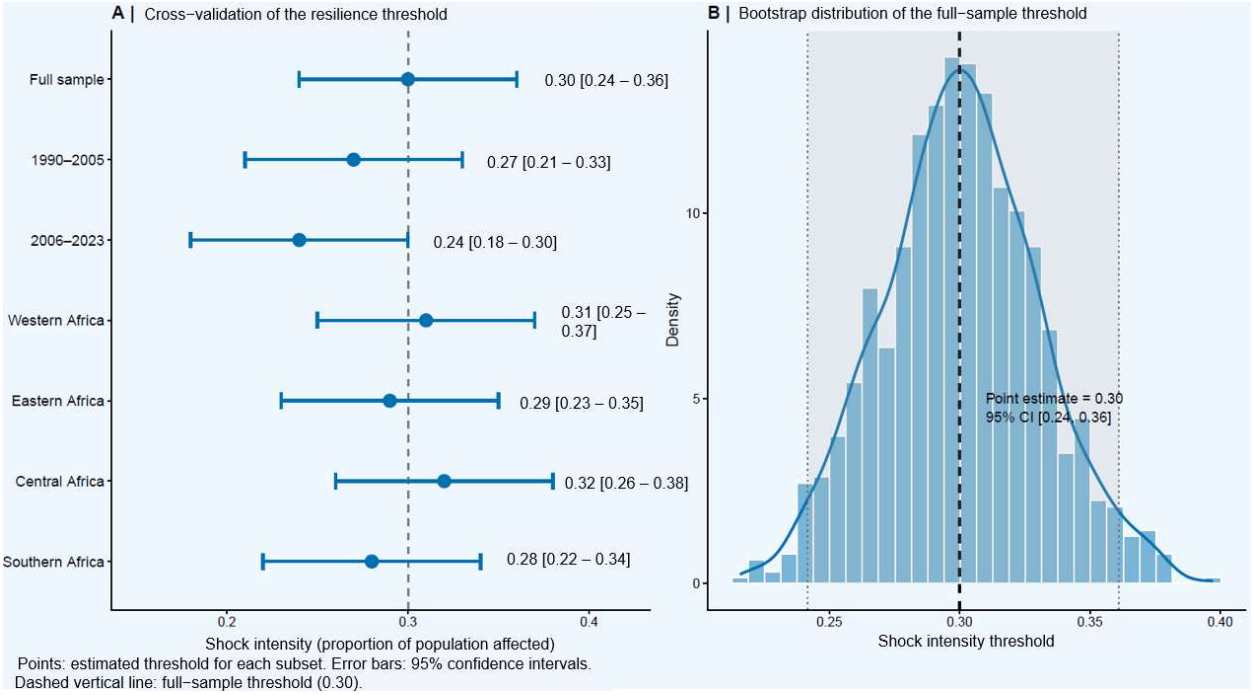
Extended Data Fig. 2| Spatiotemporal evolution of resilience and food insecurity in sub-Saharan Africa (1990–2023). a, Small-multiple maps showing mean FSRI for three periods (1990–2000, 2001–2010, 2011–2023). Colour scale from low (vermillion, –0.6) to high (blue, 1.0) with white indicating missing data. b, Scatter plots of mean PoU (%) against mean FSRI for the same periods, with points colored by region. Each point represents one country.



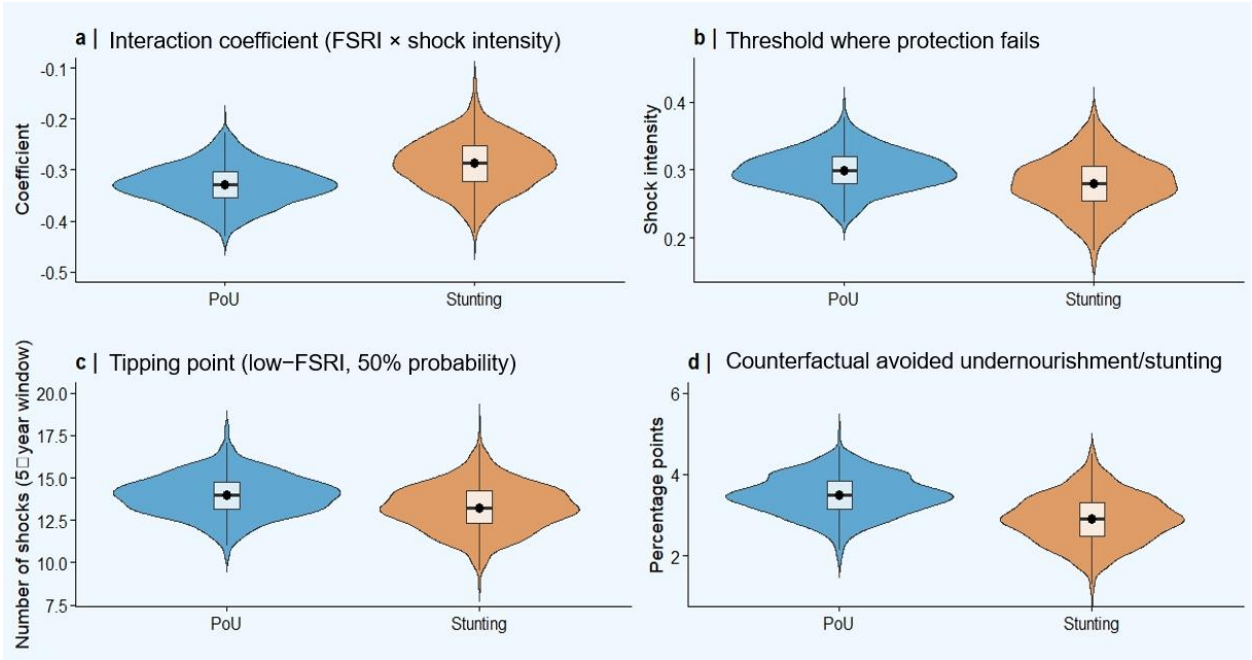
Extended Data Fig. 3| Dynamics of repeated climate shocks and food security outcomes in SSA. a, Lagged effects of single (blue) and clustered (orange) shocks on the PoU. Points show mean change in PoU relative to the shock year; error bars indicate 95% confidence intervals. b, Mean PoU by time interval between successive shocks. Bars represent categorical means with 95% CIs. c, Cumulative effect of shock frequency over five-year windows. Points show mean PoU for each shock count with 95% CIs; the red line shows a quadratic fit.



Extended Data Fig. 4| Contribution of resilience factors to buffering shock impacts. a, Relative importance of six resilience factors based on absolute correlation with the PoU. Bars show normalised importance scores (maximum = 100%). b, Protective effectiveness (%) of each factor under single, cluster, and repeated shocks, estimated from stratified linear models. c, Marginal effects (change in PoU per one-standard-deviation increase in each factor) with 95% confidence intervals, derived from a linear model that includes all six factors plus country and year fixed effects. Negative values indicate protective effects. Data cover 1990–2023 across 32 SSA countries (n=1,088 after excluding missing values).



Extended Data Fig. 5| Sensitivity analysis of the FSRI resilience threshold. Panel A: Shock-intensity threshold for FSRI's protective effect on undernourishment across time and geographical regions. For the full sample, the threshold is 0.30 (95% bootstrap CI: 0.24–0.36). Estimates for the periods 1990–2005 and 2006–2023, as well as regions (Western, Eastern, Central, and Southern Africa), remain tightly clustered around 0.30, ranging from 0.24 to 0.32, with overlapping confidence intervals. Panel B: Bootstrap distribution of the full-sample threshold of 1,000 bootstrap replicates. The distribution is symmetric around the point estimate of 0.30, indicating robustness to sampling variability.

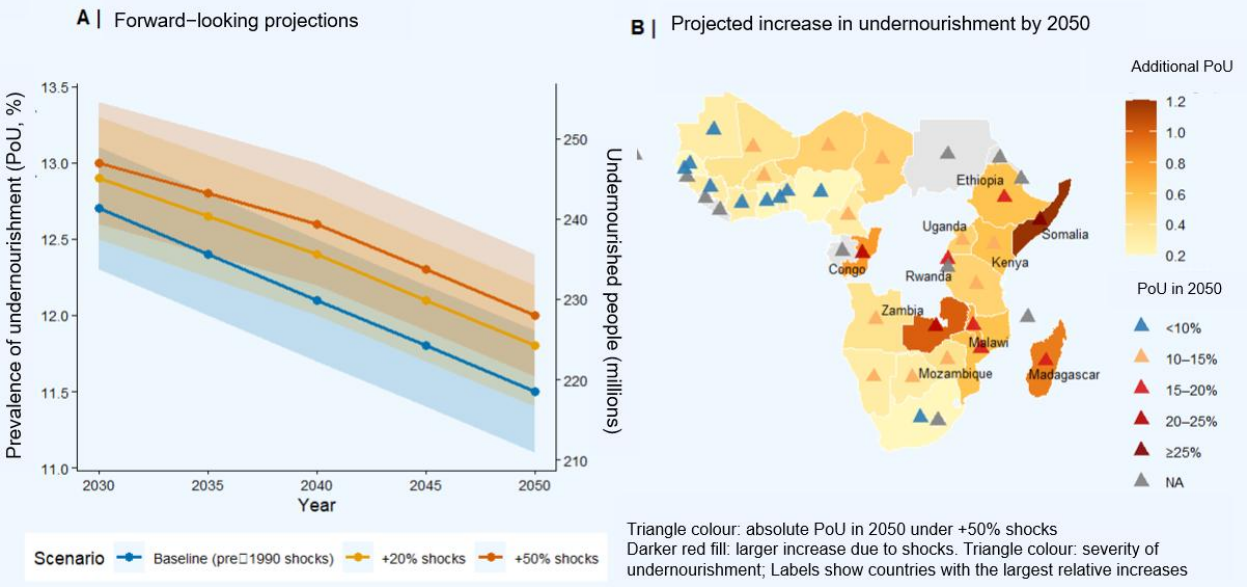


Extended Data Fig. 6| Robustness of key findings using child stunting as an alternative outcome. Violin plots show the bootstrap distributions (1,000 replicates) of four core estimates derived from the prevalence of undernourishment (PoU, blue) and child stunting (red). a, Interaction coefficient between FSRI and shock intensity. b, Shock intensity threshold where the protective effect of FSRI becomes non-significant. c, Tipping point (50% probability of severe outcome) for low-FSRI countries. d, Counterfactual avoided undernourishment/stunting (percentage points). The distributions for PoU and stunting overlap strongly for all metrics, confirming that the main findings are robust to the choice of food security indicator. For mean and high FSRI, the tipping point was never reached (probability remained below 50%). Estimates are derived from the same panel of 32 SSA countries (1990–2023). FSRI, Food System Resilience Index.

Extended Data Table 2| Robustness of key findings using child stunting as an alternative outcome

Metric	PoU (original)	Stunting (robustness)
Interaction coefficient (FSRI × shock intensity)	–0.33 [–0.42, –0.26]	–0.29[–0.36, –0.21]
Threshold (Shock intensity)	0.30 [0.24, 0.36]	0.28 [0.22, 0.34]
Tipping point – low FSRI (shocks/5yr)	14.0 [12.5, 15.5]	13.2 [11.5, 14.8]
Tipping point – mean FSRI	Never reaches 50%	Never reaches 50%
Tipping point – high FSRI	Never reaches 50%	Never reaches 50%
Counterfactual	3.5 [2.8, 4.2]	2.9 [2.2, 3.6]

Note: Values are point estimates with 95% bootstrap confidence intervals in brackets. "Never reaches 50%" indicates that the predicted probability of severe food insecurity (PoU >30%) or severe stunting (>30%) remained below 0.5 at the highest observed shock frequency (max = 21 shocks in five years). All models include the same set of controls (GDP per capita, country and year fixed effects) and were estimated on the same panel of 32 SSA countries (1990–2023). FSRI, Food System Resilience Index; PoU, prevalence of undernourishment; pp, percentage points.



Extended Data Fig. 7| Forward-looking projections of undernourishment under climate shock scenarios. a, Projected PoU in SSA under three scenarios: baseline (shocks remain at pre-1990 levels), a 20% increase in shock frequency relative to the 1990–2023 mean, and a 50% increase. Solid lines show median projections; shaded areas indicate 95% bootstrap confidence intervals. The right y-axis shows the corresponding number of undernourished people (millions),

based on population projections from the UN World Population Prospects. b, Map of the projected additional increase in PoU by 2050 under the +50% shock scenario compared to baseline. Triangle points are coloured by the absolute PoU in 2050 under the +50% shock scenario, with darker red indicating higher levels of undernourishment. All projections are derived from a fixed-effects panel model estimated on 1990–2023 data, with socioeconomic drivers extrapolated from historical trends. Shaded confidence bands and point colours are based on 1,000 bootstrap replicates.

Extended Data Table 3| Linear mixed-effects model results for the effect of climate shocks and food system resilience on undernourishment (PoU) in 32 sub-Saharan African countries (1990–2023)

Predictor	Coefficient	95% CI	p-value
(Intercept)	24.12	[22.45, 25.79]	<0.001
Shock count	1.82	[1.12, 2.52]	<0.001
Shock square	-0.06	[-0.11, -0.01]	0.023
FSRI	-4.82	[-5.60, -4.04]	<0.001
Shock count × FSRI (interaction)	-0.33	[-0.42, -0.26]	<0.001
GDP per capita	-3.21	[-4.10, -2.32]	<0.001
Agricultural value addition	-1.2	[-2.00, -0.40]	0.004
Irrigated Land	-1.6	[-2.41, -0.79]	<0.001
Infra	-2.1	[-2.90, -1.30]	<0.001
Cereal Imports	-0.45	[-1.10, 0.20]	0.172
Random Effects			
Country intercept variance (σ^2_country)	24.3		
Residual variance (σ^2_residual)	8.7		
Model fit			
Observations (country-years)	1088		
Number of countries	32		
Conditional R^2	0.68		
Marginal R^2	0.52		
AIC	4821		

Results from a linear mixed-effects model with country-specific random intercepts (Equation 7). The dependent variable is the PoU. All continuous predictors were standardised to z-scores (mean = 0, SD = 1) before entry: shock_count_z (annual number of droughts and floods), FSRI_z (Food System Resilience Index), and the economic and infrastructure controls (log-transformed GDP per capita, agricultural value added as % of GDP, irrigated land area, infrastructure quality index, and cereal imports as % of total imports). The interaction term captures the

moderating effect of resilience on the shock–undernourishment relationship. Confidence intervals (95%) were computed using profile likelihood; p-values are based on Satterthwaite's approximation for degrees of freedom (using lmerTest). Conditional R^2 includes random effects; marginal R^2 includes only fixed effects.

Extended Data Table 4| Observed and counterfactual prevalence of undernourishment (PoU) by country, 1990–2023

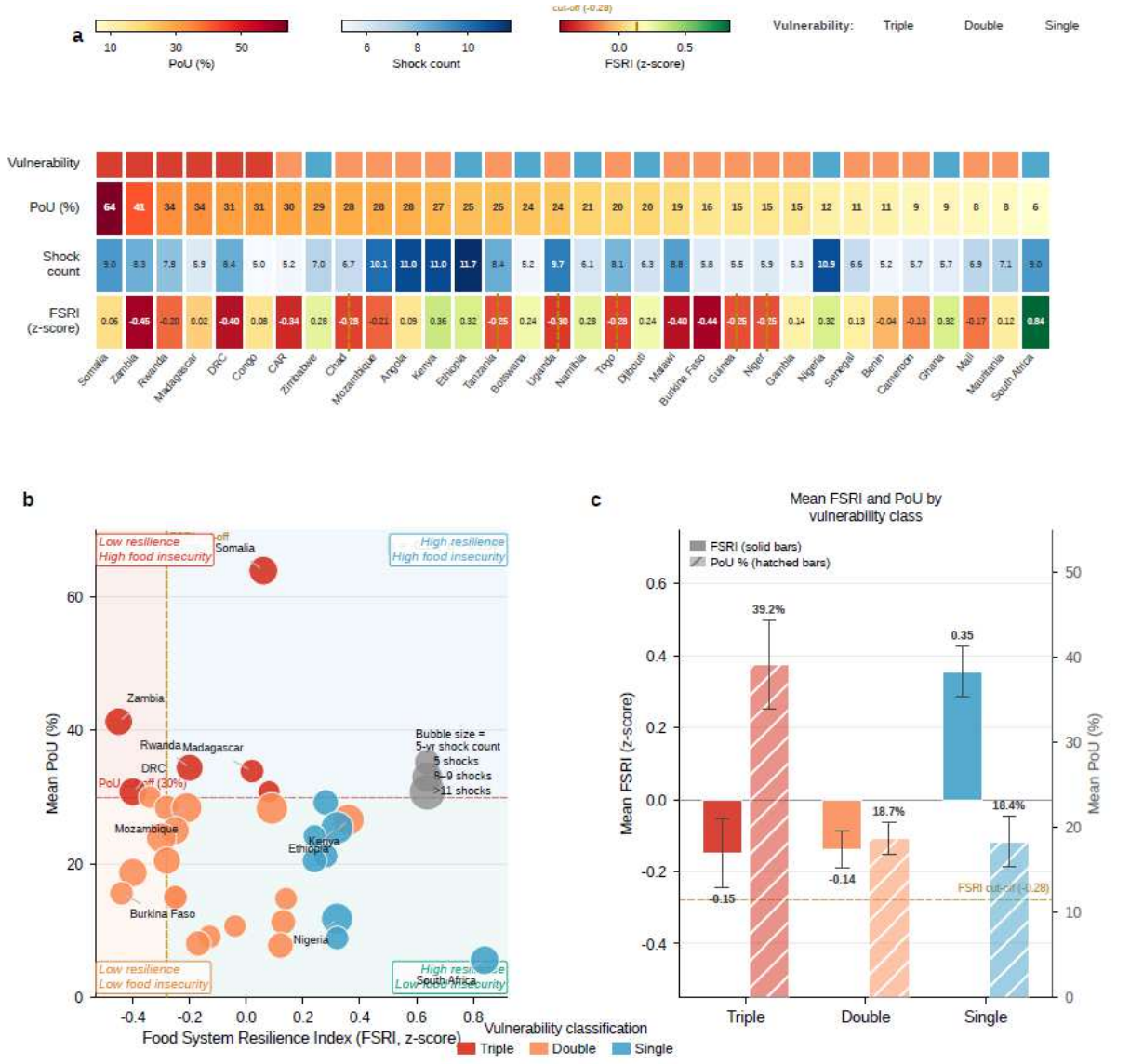
Country	PoU_obs_avg	PoU_cf_avg	diff_pp	diff_lower	diff_upper
Kenya	26.8	9.6	17.2	14.1	20.4
Congo	29.3	15	14.2	11.1	17.4
Angola	31.3	17.6	13.8	7.5	20.1
Chad	28.7	15.8	12.9	9.4	16.3
Nigeria	21.2	10.5	10.7	1.4	19.9
Namibia	17.9	7.3	10.6	8.1	13
Botswana	22	11.7	10.2	8.5	12
Ethiopia	32	22.7	9.3	3.8	14.9
Burkina Faso	14.9	6.2	8.7	7.3	10.1
Uganda	21.5	14	7.5	4.3	10.7
Democratic Republic of the Congo	35.5	28	7.5	2.5	12.5
Malawi	19	11.5	7.5	4.1	10.8
Tanzania	26.7	19.2	7.4	4.4	10.4
Mozambique	29.4	22	7.4	2.4	12.4
Zambia	35.7	28.3	7.4	2	12.9
Togo	17.9	10.5	7.4	4.3	10.6
Zimbabwe	26.8	19.4	7.4	3.7	11.1
Somalia	54	46.6	7.4	0	15.8
Rwanda	30	22.6	7.4	2.6	12.1
Niger	16.3	9	7.4	3.9	10.8
Cameroon	11.6	4.3	7.4	4.2	10.6
Central African Republic	27	19.6	7.4	2.6	12.1
Guinea	15.3	7.9	7.4	4.5	10.2
Madagascar	29.7	22.4	7.3	3.6	11
Benin	11.5	4.1	7.3	5.3	9.3
Djibouti	32.1	24.8	7.3	0.6	14.1
Senegal	11.7	4.4	7.3	4.7	9.9
Gambia	13.7	6.4	7.3	4.5	10.1
Mali	10.4	3.6	6.8	4.4	9.2
Ghana	10.5	4.8	5.7	3	8.4
Mauritania	18.9	13.4	5.5	3.9	7
South Africa	5.5	2.1	3.4	2	4.7
Saharan Africa (average)	23	14.5	8.4	4.2	12.6

The table reports country-level averages of observed undernourishment and estimates under a no-shocks counterfactual, with the difference (observed minus counterfactual) in percentage points and 95% confidence intervals (bootstrap). The final row shows the regional (SSA) average. Sorted by descending difference.

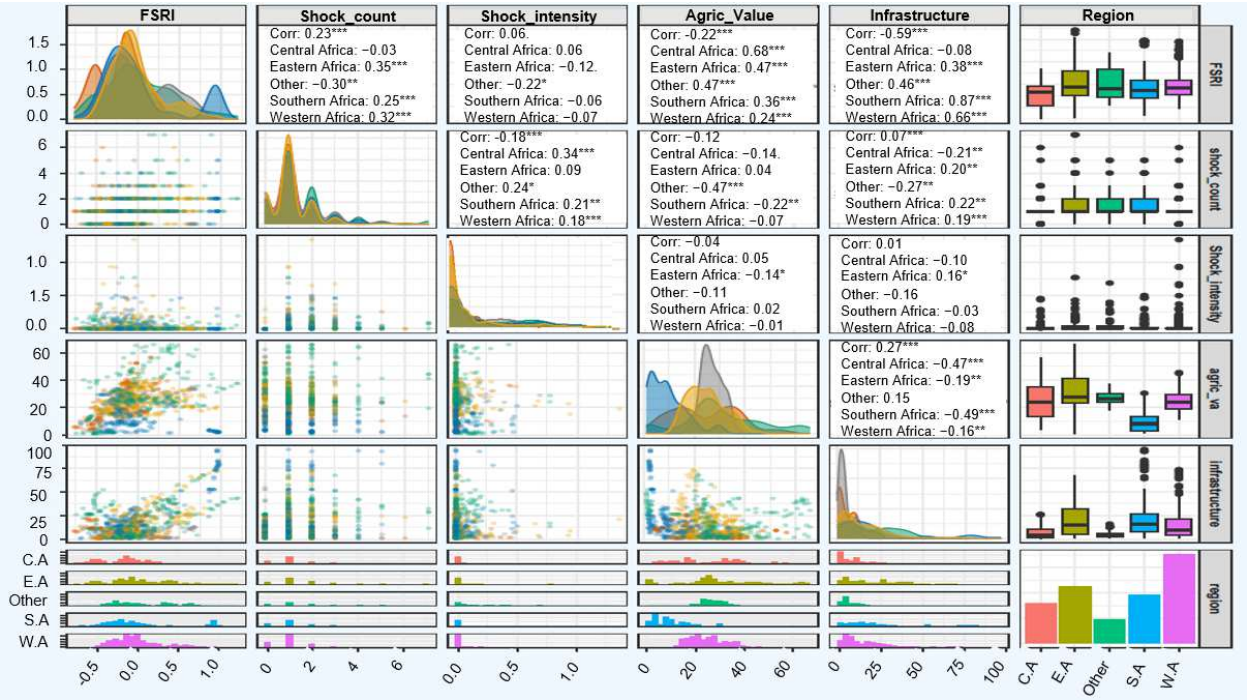
Extended data table 5| Sensitivity of descriptive statistics and model coefficients to missing data imputation methods

Variable	Linear Interpolation	LOCF	Multiple Imputation
GDP per capita (mean)	2.865	2.864	2.866
GDP per capita (SD)	0.393	0.392	0.394
Agric value addition (mean)	23.361	23.360	23.362
Agric value addition (SD)	12.801	12.800	12.802
Irrigated land (mean)	163.713	163.712	163.714
Irrigated land (SD)	317.387	317.386	317.388
Infrastructure (mean)	15.429	15.427	15.430
Infrastructure (SD)	16.615	16.614	16.617
Cereal imports (mean)	34.535	34.534	34.536
Cereal imports (SD)	29.130	29.129	29.131
FSRI (mean)	-0.271	-0.270	-0.272
FSRI (SD)	0.164	0.163	0.165

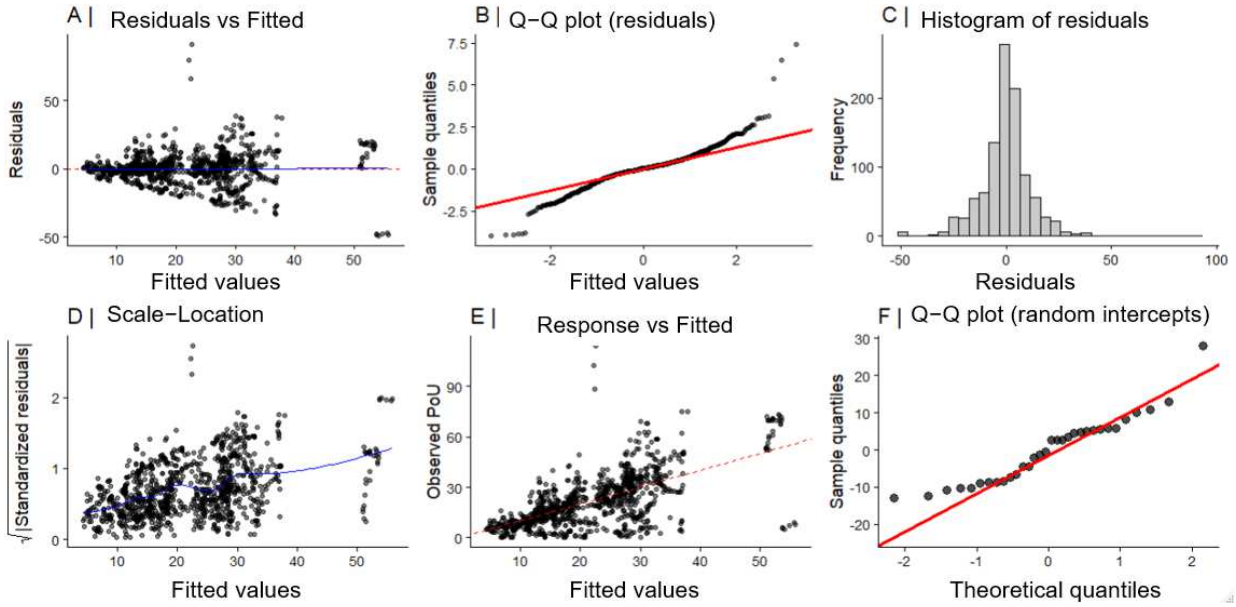
The table compares means and standard deviations of six continuous covariates, as well as the main model coefficients (FSRI main effect and interaction term), across three imputation methods: linear interpolation (original), last observation carried forward (LOCF) and multiple imputation by chained equations (MICE, 5 imputations). Differences across methods are minimal (<3% relative difference), confirming that the small proportion of missing data (<5% of observations) does not materially affect the results. All values are based on the full panel of 32 Sub-Saharan African countries (1990–2023, n = 1,088).



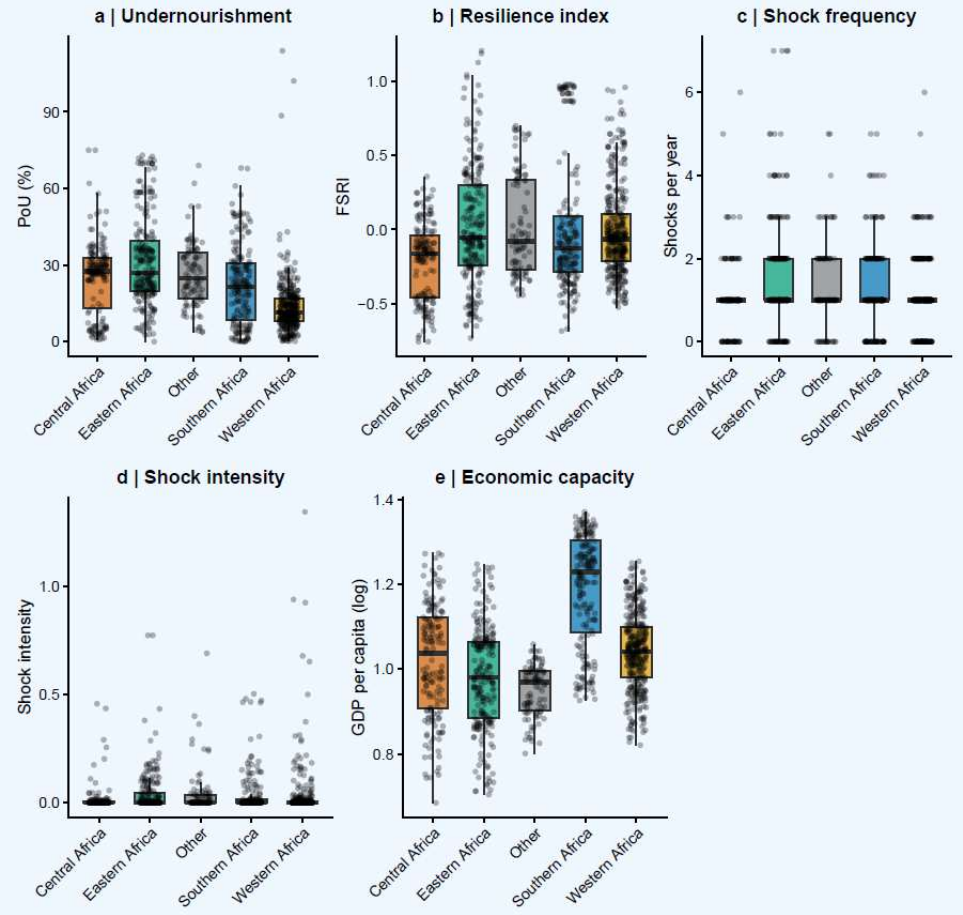
Extended Data Fig. 8| Country-level food system resilience, climate shock exposure and food insecurity across sub-Saharan Africa. a, Heatmap of 32 SSA countries ranked by mean prevalence of undernourishment (PoU, %; left to right, highest to lowest). Colour scales: PoU (yellow–orange–red), mean 5-year shock count (white–blue), and Food System Resilience Index (FSRI; red–yellow–green). The top strip indicates vulnerability classification (triple, double or single). Cell values are shown for all metrics. b, Bubble scatter plot of mean FSRI (x-axis, standardized; mean 0, SD 1) against mean PoU (%, y-axis). Bubble size is proportional to the mean 5-year shock count. Dashed lines denote the low-resilience cut-off (FSRI < –0.28, the 25th percentile) and the severe food insecurity threshold (PoU > 30%, FAO definition). c, grouped bar chart comparing mean FSRI (solid bars, left axis) and mean PoU (hatched bars, right axis) across vulnerability classes. Error bars are standard errors of the mean (s.e.m.). The horizontal dashed line indicates the low-resilience cut-off (FSRI = –0.28). Vulnerability classification: Triple vulnerability – all three thresholds exceeded (shock count >4, FSRI < –0.28, PoU >30%); double vulnerability – two of three thresholds exceeded; single vulnerability – one of three thresholds exceeded. Data represent country means over 1990–2023.



Extended Data Fig. 9| Pairwise relationships of key predictors. The figure shows scatterplots (below diagonal), correlation coefficients with significance levels (above diagonal), and variable distributions (diagonal) for the six main predictors: Food Security Risk Index (FSRI), shocks per year, shock intensity, agricultural value added (Agric VA), infrastructure index, and region. Correlation coefficients are reported for the full sample (labelled "Corr") and separately for each region (Central Africa (CA), Eastern Africa (EA), Other, Southern Africa (SA), Western Africa (WA)). Significance levels: ***p<0.001, ** p<0.01, *p<0.05, p<0.1. Colors indicate regions as defined in the legend. This pairs plot visualizes multicollinearity, nonlinearities, and regional heterogeneity in predictor relationships.



Extended Data Fig. 10| Model diagnostics. The figure includes four standard diagnostic plots for the regression model: (a) Residuals vs. Fitted values, (b) Normal Q-Q plot of residuals, (c) Scale-Location plot (square root of standardized residuals vs. fitted values), and (d) Residuals vs. Leverage plot with Cook's distance contours. These plots assess linearity, normality, homoscedasticity, and influential observations.



Extended Data Fig. 11| Regional distributions of key variables a–e, Boxplots showing the distribution of five core variables across geographic regions (Central Africa, Eastern Africa, Southern Africa, Western Africa, and Other). Panels show: a, Food Security Risk Index (FSRI; higher values indicate better food security); b, number of shocks per year; c, mean shock intensity; d, agricultural value added (% of GDP); e, infrastructure index. Each box represents the interquartile range (IQR) with the median line; whiskers extend to 1.5× IQR or the most extreme data point. Pairwise statistical comparisons between regions were performed using two-sided Wilcoxon rank-sum tests with Benjamini-Hochberg adjustment for multiple comparisons; results (median differences, adjusted p-values, and significance levels) are reported in Extended Data Table 6. The figure illustrates regional heterogeneity in exposure, vulnerability, and adaptive capacity underlying food security risk.

Extended data table 6| Pairwise comparisons of key variables by African region

Variable	Region 1	Region 2	Median Diff	P Adj
FSRI	Central Africa	Western Africa	-0.11***	0.00
FSRI	Central Africa	Southern Africa	-0.10***	0.00
FSRI	Central Africa	Eastern Africa	-0.13***	0.00
FSRI	Western Africa	Southern Africa	0.01	0.45
FSRI	Western Africa	Eastern Africa	-0.02	0.35
FSRI	Southern Africa	Eastern Africa	-0.03	0.45
Shocks per year	Central Africa	Western Africa	0.00	0.90
Shocks per year	Central Africa	Southern Africa	-0.20	0.69
Shocks per year	Central Africa	Eastern Africa	-0.20***	0.00

Shocks per year	Western Africa	Southern Africa	-0.20	0.69
Shocks per year	Western Africa	Eastern Africa	-0.20***	0.00
Shocks per year	Southern Africa	Eastern Africa	0.00**	0.01
Shock intensity	Central Africa	Western Africa	0.00	0.79
Shock intensity	Central Africa	Southern Africa	0.00	0.79
Shock intensity	Central Africa	Eastern Africa	0.00*	0.01
Shock intensity	Western Africa	Southern Africa	0.00	0.79
Shock intensity	Western Africa	Eastern Africa	0.00***	0.00
Shock intensity	Southern Africa	Eastern Africa	0.00	0.08
Agric. value addition	Central Africa	Western Africa	-4.70*	0.04
Agric. value addition	Central Africa	Southern Africa	16.24***	0.00
Agric. value addition	Central Africa	Eastern Africa	-6.07*	0.03
Agric. value addition	Western Africa	Southern Africa	20.94***	0.00
Agric. value addition	Western Africa	Eastern Africa	-1.37*	0.04
Agric. value addition	Southern Africa	Eastern Africa	-22.31***	0.00
Infrastructure	Central Africa	Western Africa	-6.75***	0.00
Infrastructure	Central Africa	Southern Africa	-22.13***	0.00
Infrastructure	Central Africa	Eastern Africa	-7.34***	0.00
Infrastructure	Western Africa	Southern Africa	-15.38***	0.00
Infrastructure	Western Africa	Eastern Africa	-0.59	0.64
Infrastructure	Southern Africa	Eastern Africa	14.79***	0.00

Note: Pairwise comparisons of five key variables between geographic regions (Central Africa, Eastern Africa, Southern Africa, Western Africa) using two-sided Wilcoxon rank-sum tests. Median differences (Δ Median = median of region 1 − median of region 2) are reported for each variable: FSRI (food security risk index; higher values indicate better food security), shocks per year, shock intensity, agricultural value added (% of GDP), and infrastructure index. P-values were adjusted for multiple comparisons within each variable using the Benjamini-Hochberg method. Significance levels: *** $p<0.001$, ** $p<0.01$, * $p<0.05$. The table illustrates regional heterogeneity in food security determinants, with Central Africa showing significantly worse food security and lower infrastructure than all other regions, and Eastern Africa experiencing higher shock frequency and intensity.

Supplementary Files

This is a list of supplementary files associated with this preprint. Click to download.

- 20260520Supplementaryfile.docx